RSC Advances

REVIEW

View Article Online
View Journal | View Issue

Cite this: *RSC Adv.*, 2025, **15**, 21341

Stability and application of TiO_2 nanomaterials in aqueous suspensions: a review

Ljiljana Spasojević, [ab] Irena Ivanišević *[a] and Maja Dutour Sikirić *[a]

Excellent photo-physical, photo-chemical, and surface properties, which enable them to be used in a wide range of applications, make TiO_2 nanomaterials (TiNMs) among the most extensively investigated and commercially utilized nanomaterials. In many applications, TiNMs are used in the form of suspensions. Therefore, understanding their dispersibility and colloidal stability is crucial. Despite a large number of investigations into the colloidal stability of TiNMs, the preparation of stable suspensions and the choice of suitable dispersants still rely on trial and error. Motivated by this, in this review, we present and discuss the versatility of dispersants for stabilizing TiNMs. The investigations are discussed within the framework of DLVO theory, which, despite its limitations, provides a theoretical foundation for understanding the observed effects. In addition, tested and commercial applications are briefly discussed.

Received 10th April 2025
Accepted 18th June 2025

DOI: 10.1039/d5ra02499d

rsc.li/rsc-advances

1. Introduction

Titania nanomaterials (TiNMs) are nowadays among the most extensively engineered nanomaterials, incorporated in numerous consumer and industrial products.[1] Titania-based nanostructures are being utilized for diverse applications due to their unique energy band gap and quantum efficiency, highlighting their photo-physical, photo-chemical and surface properties. Because of that, TiNMs are significantly used in catalytic reactions (reduction of nitrogen oxides to elemental nitrogen,[2] antibiotic degradation[3]), photochemical and photo-physical applications (photodegradation of pollutants, water remediation, hydrogen production, self-cleaning surfaces, antimicrobial coatings),[4–7] (bio)medicine (drug-delivery systems, treatment of cancer),[8,9] as an additive in ceramics,[10,11]

[a]*Laboratory for Biocolloids and Surface Chemistry, Division of Physical Chemistry, Ruđer Bošković Institute, Bijenička cesta 54, 10000 Zagreb, Croatia. E-mail: Irena.Ivanisevic@irb.hr; sikiric@irb.hr*

[b]*Department of Applied and Engineering Chemistry, Faculty of Technology Novi Sad, University of Novi Sad, Bul. cara Lazara 1, 21000 Novi Sad, Serbia. E-mail: lj.spasojevic@tf.uns.ac.rs*

Ljiljana Spasojević

Dr Ljiljana Spasojević is a Research Associate at the Faculty of Technology Novi Sad, University of Novi Sad, Serbia, where she obtained her PhD in Food Engineering at the Department of Applied and Engineering Chemistry in 2021. Since joining the faculty in 2016, she has published 17 peer-reviewed papers (H-index 9, 284 citations), delivered two invited lectures, and completed a one-year postdoctoral fellowship at the Ruđer Bošković Institute in Zagreb, Croatia. Her research focuses on colloidal systems, nanoparticles, and thin films, with industrial applications. She has also contributed to several domestic and international scientific and R&D projects.

Irena Ivanišević

Irena Ivanišević obtained her PhD in Inorganic Chemistry from the University of Zagreb Faculty of Chemical Engineering and Technology in 2020. Her doctoral research focused on the synthesis and characterization of silver nanoparticles for the fabrication of inkjet-printed electrochemical (bio)sensors. Currently, she is a Postdoctoral researcher in the Laboratory for Biocolloids and Surface Chemistry at the Ruđer Bošković Institute, Zagreb, Croatia, under the supervision of Dr Maja Dutour Sikirić. Her current scientific interest involves investigating the stability of TiO_2 suspensions and developing antimicrobial TiO_2 coatings for biomedical applications. She has co-authored 15 peer-reviewed publications indexed in Scopus and Web of Science Core Collection.

paint pigments,[12] cement composites[13] and polymer filler,[14] medical applications,[15,16] food[17] and in cosmetics as a UV absorber.[17–19] Therefore, it is not surprising that global market analyses predict a twofold growth in the value of the TiNMs market over the next nine to ten years.[20]

As for other nanomaterials, the properties of nanosized titania materials differ significantly from their bulk counterparts.[21] As the particle size decreases, a larger fraction of atoms is located at the surface relative to the bulk, creating numerous reactive sites that enhance chemical interactions with the surroundings. Additionally, the high surface-to-volume ratio and disruption of the periodicity of the lattice symmetry at the surface alter the electronic structure of TiNMs, resulting in novel quantum effects.[22] Furthermore, the reduced particle size has a significant impact on the mobility in dispersions, which is mainly controlled by Brownian motion.[23] However, like other nanoscale materials, small titania particles have a strong tendency to aggregate spontaneously and eventually settle, thereby reducing their surface energy. This process can have a negative impact on the final TiNMs applications and must, therefore, be avoided.

Since the majority of chemical, biological, and environmental processes occur in wet conditions, the dispersibility of TiNMs in solvents of varying polarity is a fundamental aspect to consider.[24,25] To fully understand how these nanomaterials are dispersed in a liquid medium, it is essential to investigate the formation and properties of the solid–liquid interface. In general, various forces act on nanomaterials (NMs) in a liquid medium and determine their stability – attractive van der Waals forces (vdW), repulsive forces resulting from the electrical double layer (EDL) surrounding the particle, hydrophilic/hydrophobic interactions, and steric, electrostatic and electrosteric forces as a result of the particle surface coating. To predict the stability of nanomaterial suspensions, the DLVO theory, which considers only attractive van der Waals and repulsive electrostatic double layer forces, is most commonly used, despite its drawbacks.[26] Since many properties of the final product strongly depend on the colloidal stability of the particles, the dispersibility of nanopowders in a liquid medium remains a significant challenge and a focus of extensive scientific research.

Suspensions are heterogeneous systems in which fine particles are uniformly distributed in a continuous liquid phase and do not dissolve.[27] The dispersion of TiNMs typically involves three key steps: wetting of the nanomaterial surfaces, mechanical dispersion (often achieved through ultrasonic treatment), and stabilization of the resulting colloidal suspension.[28] Wetting, *i.e.* the ability of liquids to remain in contact with solids, is a direct result of the intermolecular interactions that occur at the solid/liquid interface. After the wetting step, mechanical dispersion is employed to achieve complete separation of the particles. Once dispersed, maintaining long-term stability is crucial. This is usually achieved through the use of surface activators and/or dispersants.[29]

Over the last decades, many studies have focused on the TiNMs dispersion stability in water[30,31] and organic solvents,[32,33] using a broad spectrum of chemical species as particle stabilizers: surfactants,[34] polyelectrolytes and copolymers,[35,36] organic acids,[37] and small inorganic species.[38] In addition, numerous studies have been conducted to study the impact of ultrasonication,[39–41] nanoparticle concentration,[41] ionic strength (IS), and pH.[42,43] Furthermore, a large number of review papers on titania nanomaterials have been published, focusing on synthetic nanomaterial approaches,[4,5,11,22,44] classification and material applications,[44] photocatalytic activity,[45] functionalized textile surfaces,[46] wastewater remediation,[6] antimicrobial coatings,[47,48] indoor air purification,[49] volatile organic compounds (VOCs) sensor,[50] medical applications,[16] food and personal care products,[17,51] toxicology and environmental impact[52,53] providing insight into a broad spectrum of titania nanomaterials applications. This can be evidenced by the exponential growth in the number of scientific and review papers that are based, at least in part, on the colloidal stability of TiNMs (Fig. 1).

However, to the best of our knowledge, only Faure *et al.*[24] have reviewed the stability of suspensions of TiNMs for

Maja Dutour Sikirić

Maja Dutour Sikirić earned her PhD in physical chemistry from the Faculty of Sciences at the University of Zagreb, Croatia, in 2002. Currently, she is Scientific Advisor at the Division of Physical Chemistry, Ruđer Bošković Institute, Zagreb, Croatia. Her current research interests focus on the influence of different types of nanomaterials on the formation of calcium phosphates with the aim of producing multifunctional materials for orthopaedic applications, nanomaterials-based antimicrobial coatings for different applications, as well as investigations of the stability of inorganic and soft nanoparticles in various matrices relevant to biomedical applications and environmental protection.

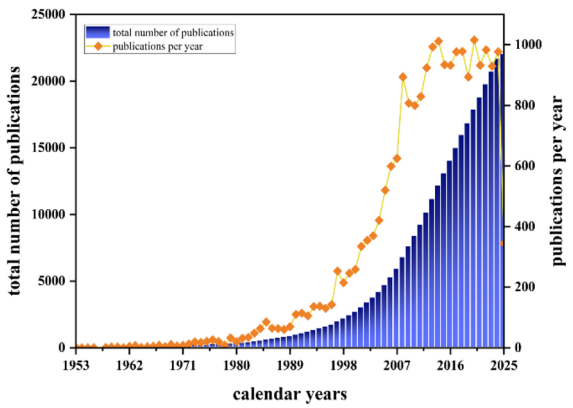

Fig. 1 Number of publications per year and cumulative publications regarding TiO_2 nanomaterials' colloidal stability. Determined from Scopus platform using keywords: "titanium dioxide OR titania OR TiO_2 OR anatase OR rutile (title) and suspension* OR dispersion* OR colloid*".

transparent photocatalytic and UV-protecting coatings and sunscreens. The aim of this paper is, therefore, to provide a comprehensive overview of the colloidal behaviour of nano-sized titania materials in aqueous media in terms of particle size, particle size distributions, and zeta potential values, taking into account the effects of TiNMs concentration, nature of stabilizing agents (surfactants, polymers, small organic and inorganic molecules and natural organic molecules) and their concentrations, as well as the effects of the type of homogenization method, solution chemistry parameters (influence of ionic strength and pH of the media) and their versatile applications.

The review starts with a description of TiNMs, their crystal structure, and methods of synthesis. A short description of DLVO theory and aggregation processes follows. The versatility of dispersants for stabilizing TiNMs is then examined and discussed in detail, including the stability of pristine TiNMs suspensions and colloidal stability in the presence of surfactants, polymers, small organic and inorganic molecules, and natural organic matter (NOM). In the final section of the paper, the application of stable TiNMs suspensions in the preparation of photocatalytic coatings, self-cleaning coatings on textiles, antibacterial surface coatings, additives for enhancing lubrication, and tribological properties of pure water, solar cells, and pigments is briefly discussed.

2. Titanium dioxide nanomaterials

2.1. Titanium dioxide crystal structure

Titanium dioxide (TiO_2) occurs in at least eleven crystalline forms, of which anatase, brookite, rutile, and TiO_2(B) (Fig. 2) are the most frequently encountered as they are stable at ambient or low pressure.[54] Anatase and rutile, which are thermodynamically stable at low and high temperatures, respectively, are widely employed in photocatalysis and pigment production. In contrast, brookite and TiO_2(B) are metastable, rarely found in nature, and challenging to synthesize in pure form.[55] Although all forms share the same TiO_2 stoichiometry, their crystal structures differ significantly. The base building block of all TiO_2 phases is a Ti–O polyhedra; in the case of low-pressure phases, the $[TiO_6]^{2-}$ octahedra. The variations in the three-dimensional arrangement, in particular, whether the octahedra share corners, edges, or a combination of both, give rise to distinct crystalline structures. For example, the structures of rutile, brookite, and anatase differ in the number of shared octahedral edges. In rutile 2, brookite 3, and in anatase 4 out of 12 $[TiO_6]^{2-}$ octahedra edges are shared.[54,56]

Interestingly, despite similar Ti–O bond lengths in all polymorphs, the O–O distances between adjacent and non-sharing octahedra differ substantially.[58] These structural variations influence the mass density and electronic band structure of the nanomaterial, thereby affecting the physicochemical and optoelectronic properties that are crucial to the applications.[59]

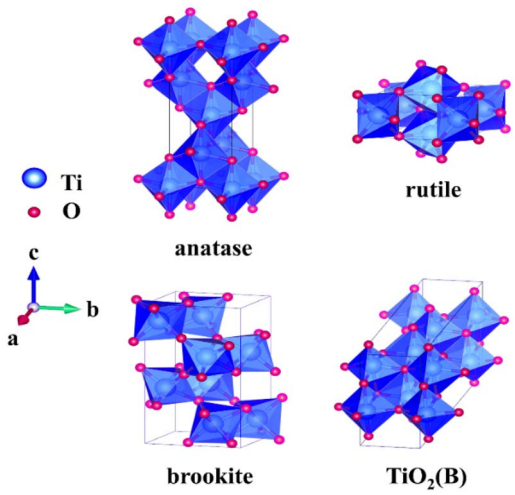

Fig. 2 Crystal polymorphs of TiO_2. Crystal structures taken from The Materials Project website (https://next-gen.materialsproject.org/about/cite) and displayed in VESTA.[57]

2.2. Synthesis of TiO_2 nanomaterials

Numerous methods suitable for the synthesis of titania nanostructures have been developed, including the solvothermal/hydrothermal method, sol–gel synthesis, micelle and inverse micelle method, microemulsion method, laser pyrolysis, and laser ablation, chemical and physical vapor deposition, electrodeposition, electrospinning, sonochemical method, microwave assisted synthesis, ball milling, direct oxidation method, spray pyrolysis.[4,5,60–62] Nowadays, eco-friendly, high-productive, and cost-effective methods utilizing microbial or plant extracts or other biological sources are preferred for the efficient production of TiNMs.[60,62–64] In general, all the above methods can be summarized in two different synthetic approaches: (i) top-down, in which mechanical force is applied to break down the bulk material into the nanosized entities, and (ii) bottom-up, in which the functional nanomaterial is prepared using atomic building blocks.[65–67] Each approach renders a variety of nanostructures that differ in size, morphology, and dimensionality at the nanoscale (0D – particles, 1D – wires, 2D – layers and sheets, or 3D architectures), crystalline form, and surface area.[68–70] Different morphologies, such as nanorods, nanotubes, or nanowires, offer varying degrees of surface area-to-volume ratios and may express different crystal facets, which can significantly influence the activity of titania materials for their intended applications and affect their dispersibility. The differing shapes may hinder agglomeration; for example, the anisotropic shape of nanorods can lead to less favourable packing of the titania nanoparticles, *i.e.*, causing steric hindrance and resulting in an overall weaker interaction than that of nanospheres.[71]

3. Colloidal stability of nanomaterials suspensions

3.1. Colloidal stability

The theoretical framework for describing, understanding, and predicting the stability of nanomaterial suspensions is given by the DLVO theory of colloidal stability developed by Derjaguin,

Landau, Vervey, and Overbeek.[72,73] According to DLVO theory, the stability of the suspension in question depends on the interplay of two contributions: attractive van der Waals forces ($W_{vdW}(d)$) and repulsive electric double-layer interactions ($W_{dl}(d)$). DLVO theory considers that these two contributions are additive and sum to give the total energy of interaction ($W(d)$) between the particles as a function of their distance, d:[74]

$$W(d) = W_{vdW}(d) + W_{dl}(d) \quad (1)$$

van der Waals forces are short-range electromagnetic attractive forces between NPs originating from fluctuating electromagnetic fields.[25] This contribution is calculated using Hamaker theory simplified by Derjaguin approximation.[75] For the interaction of two identical spheres with radius r, $W_{vdW}(d)$ equals:[76]

$$W_{vdW}(d) = -\frac{H_{131}r}{12d} \quad (2)$$

where d is the separation distance of the spheres, and H_{131} Hamaker constant, for similar materials 1 interacting across medium 3, which defines the strength of the interaction.[74]

Around charged nanoparticles present in the electrolyte solution, an electrical double layer forms. It consists of a tightly bound counterion layer and a counterion diffusion layer in which a concentration gradient occurs.[77] The $W_{dl}(d)$ can be calculated using the mean-field Poisson–Boltzmann formalism.[76] Coupled with the Debye–Hückel approximation, this approach gives an analytical solution for low ionic strengths.[75] When two similarly charged particles approach each other, their electric double layers overlap, resulting in repulsion.[74] The charge of the particles can be estimated from the measured zeta potential, which represents the charge at the shear plane.[25] The electric double-layer interactions between spherical particles at a distance d can be calculated as:[76]

$$W_{dl}(d) = \frac{2\pi r\sigma^2}{\kappa^2\varepsilon\varepsilon_0}e^{-\kappa d} \quad (3)$$

where r is the particle radius, σ its charge, ε the dielectric constant of water, ε_0 is the permittivity of vacuum and κ the inverse Debye length.

Significant work has been conducted to extend the range of DLVO applicability, encompassing wider ranges of ionic strength and ion charges. Extended DLVO theory (XDLVO) enables the description of heteroaggregation phenomena,[78] while Sogami–Ise theory[79] improves prediction for ions with higher charges, asymmetric electrolytes, and non-spherical particles.[75]

As DLVO theory was developed for colloidal systems, it contains serious drawbacks when applied to the stability of nanoparticle suspensions, due to which correct simplifications, assumptions, and boundary conditions should be applied when interpreting the results.[80] Kovalchuk *et al.*[81] pointed out that the range of interaction between nanoparticles is larger than the radius of the nanoparticles. Consequently, the concentration at which all particles are interconnected is very low compared to colloidal systems. Therefore, at concentrations above the critical, interactions between particles become collective. Additionally, the diffusion coefficient of nanoparticles is significantly larger than that of colloidal particles.

Another drawback is that DLVO theory assumes only two types of forces. However, non-DLVO interactions such as Born repulsion (repulsion forces between atoms), hydration effects (repulsion forces arising from the tendency of hydrated particles to dehydrate in order for contact of the particles to occur), hydrophobic interaction (attractive forces arising due to the different structuring of water molecules around hydrophobic surfaces), steric interactions (stabilizing effect of polymer layer adsorbed at the surface of NP), and polymer bridging (bridging of the particles by long-chain polymers present in low concentration leading to aggregation) should also be taken into account when discussing the stability of the nanoparticles' suspension.[82]

3.2. Aggregation

The balance between attractive interparticle forces and repulsive EDL forces determines the overall aggregation rate. In general, it is considered that particles with sizes greater than 10 μm can be easily mechanically dispersed even in cases where van der Waals attraction is strong.[77] However, this is not the case for nanomaterials. As aggregation progresses, larger clusters of nanomaterials form, resulting in a non-uniform distribution of the particles, changes in their physicochemical properties, and, consequently, the sedimentation of the particles. Aggregation is thermodynamically spontaneous as it minimizes the interfacial free energy by reducing the total area of the solid–liquid interface. However, it can be slowed down kinetically by altering the solution chemistry (type of base fluid, pH value, and/or ionic strength control) and the type of dispersion/stabilization mechanism.[83]

Polymers or surfactants present in suspensions can adsorb on the surface of the nanomaterial. A formed adsorbed layer acts as a steric barrier (Fig. 3), preventing contact between particles and, consequently, their aggregation. For achieving

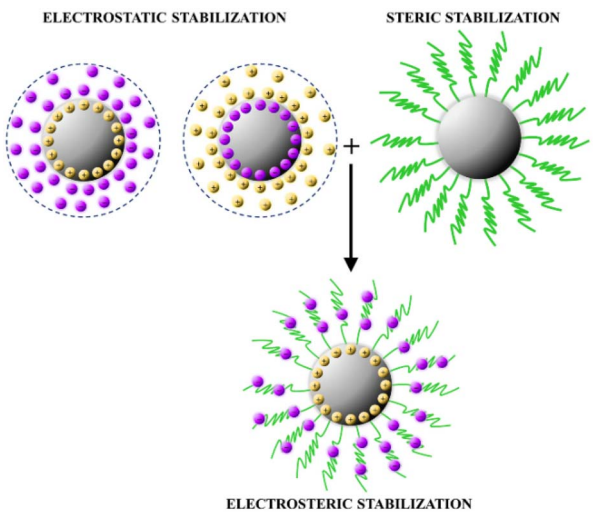

Fig. 3 Schematic representation of steric, electrostatic, and electrosteric stabilization of nanomaterials.

good stabilization, polymers of sufficient length with good adsorption properties are used.[78] Examples of such dispersants include polyvinylpyrrolidone (PVP), polyethylene glycol (PEG), and pluronic copolymers. The second type of dispersion mechanism, *i.e.*, electrostatic stabilization (Fig. 3), occurs through the coordination of ions on the surface of nanomaterials forming EDLs. The stability of the systems is achieved by repulsion of the EDLs of nanoparticles with the same charge.[78] Electrostatic stabilization will be different depending on the polarity of the base solvent. Typical examples of electrostatic stabilizers are sodium dodecyl sulphate (SDS), citrate, and poly(acrylic acid) (PAA). Electrosteric stabilization, *i.e.*, the combination of steric and electrostatic mechanisms (Fig. 3), is the most efficient way to stabilize nanoscale particles. For electrosteric stabilization, charged polymers are used. By adsorption of such polymers on the surface of charged nanoparticles, a charged steric barrier is formed. Highly charged polyelectrolytes, like poly(styrene sulfonate) (PSS), PAA, and polyethyleneimine, are used as electrosteric stabilizers.[78]

4. Dispersants investigated for stabilization of TiO_2 nanomaterials suspensions

In the design of functional nanomaterials, their architecture can be divided into two main parts – the core and the coating, *i.e.*, the stabilizing material. The core determines the size and shape, but the coating defines the physicochemical properties of the nanomaterials, which in turn determines their interaction with the environment and, thus, their overall behaviour during application. One of the essential physicochemical properties is colloidal stability in pure and mixed liquid media, at various pH values, and in the presence of salts and proteins. Nonetheless, several examples of stable suspensions prepared from bare, uncoated titania particles can also be found in the literature, and they are also included in this review (Table 1).

4.1. Pristine TiO_2 nanomaterials in aqueous media

Scientific papers summarized in this section focus on investigating suitable nanomaterial concentrations, ionic strengths, sonication parameters, and dispersion methods for preparing stable colloidal suspension of pristine, uncoated titania nanomaterials. The motivation for investigating the colloidal stability of pristine TiNMs in aqueous suspensions is twofold. On the one hand, it serves as a starting point for determining the efficacy of a specific dispersant. On the other hand, understanding the fate and behaviour of TiNMs in natural waters is crucial for their exposure-driven risk assessment, which serves as the basis for evaluating the safety of their applications.[84]

The surface of TiNMs after synthesis does not simply consist of titanium and oxygen atoms (Ti–O–Ti). The surface titania atoms are typically coordinated with amphoteric hydroxyl termination groups, which form upon the adsorption of water.

Table 1 Summary of the reviewed studies investigating the stability of aqueous suspensions of pristine TiO_2 nanomaterials (TiNMs) without the addition of dispersants

TiNMs (w/v concentration in suspension)	Homogenization method	Ionic strength	pH	Reference
Nanoparticles and nanorods, anatase (0.002%)	Sonication, 40 min	2–100 mM NaCl; 1–50 mM $CaCl_2$	3, 7	88
Nanoparticles (0.1–6.4%)	Stirring, 900 rpm, 24 h	5 mM of acetate, phosphate or carbonate buffer	2–12	89
Nanoparticles, anatase and rutile (0.002%)	Sonication, 2 h	0 and 5 mM NaCl	7	90
Nanoparticles, anatase	Vortex, 1 min, sonication, 5 min	—	—	91
Nanoparticles, rutile (0.005–0.05%)	Sonication, 20–200 min	—	—	41
Nanoparticles, anatase, sulfonated (10–50%)	Stirring 24 h, sonication 4–6 h	—	11	92
Nanoparticles doped with Er and Yb, anatase (0.1%)	Stirring 24 h, sonication 1 h	—	—	93
Nanoparticles (0.5%)	Stirring 1 min, sonication 30–180 min	—	—	39
Nanoparticles, P25	Sonication 45 min, stirring 45 min, sonication 45 min at 60 °C	—	4–6, 11	30
Nanoparticles, a mixture of anatase and brookite (0.0042%)	Stirring, 2 min	0.001 M NaCl and $CaCl_2$	4.5–8.2	43
Nanoparticles, a mixture of anatase and rutile (0.01%)	Sonication in an ice bath 10 min	Artificial fresh water 2 mM and artificial sea water 630 mM	7.5 and 8.5	84
Nanoparticles (Ag modified), (0.1–10%)	Sonication, 0–30 min	—	—	94
Nanoparticles, rutile (NM-104, Al_2O_3 coated) and anatase (E171, SiO_2 coated) (0.005%)	Sonication, 20 min	—	2–12	95

The surface hydroxyl groups (≡Ti–OH) can be protonated or deprotonated according to eqn (4) and (5):[85]

$$\equiv Ti\text{–}OH + H^+ \rightarrow \equiv Ti\text{–}OH_2^+ \quad (4)$$

$$\equiv Ti\text{–}OH + OH^- \rightarrow \equiv Ti\text{–}O^- + H_2O \quad (5)$$

When charged titania particle come into contact with an electrolyte solution, the electric double layer is formed due to the surface hydroxyl groups.[86] Among the key factors influencing the surface charge of TiNMs is the pH of the media.[87] Two pH values, related but distinct, are of interest. At the pH of the point of zero charge (pH_{PZC}), the net surface charge is equal to zero, *i.e.*, the number of positive and negative surface charges is equal. The iso-electric point (pH_{IEP}) is the pH at which the zeta potential of NMs in suspension is equal to zero.[87,96] As a result, the electrostatic repulsion for a given system is minimal.[96] Depending on the applied electrolyte and NPs properties, the pH_{IEP} for TiO_2 nanoparticles (TiNPs) ranges from 5–7.[97]

As expected, stable TiNPs aqueous suspensions can be obtained at pH 6, higher than pH_{IEP}.[30] However, reducing pH slightly below pH_{IEP} results in the aggregation of NPs,[30] but further reducing can lead to stable positively charged TINPs.[89] In addition, it was observed that the aggregation rate is higher at the initial stages of the process but decreases at later stages, which can be explained by the equilibrium between aggregate growth and breakup. An increase in TiNPs concentration also resulted in increased aggregation, as expected.[30] A study of the stability of TiNPs suspensions at pH = 2–12, obtained using HCl/NaOH solutions or different buffers, confirmed pH dependence of both zeta potential and average diameter of TiNPs aggregates in aqueous suspensions. Additionally, it was indicated that the size of TiNPs aggregates is medium-dependent at pH around 6 and differs significantly in different buffer solutions and HCl solution.[89]

Another important factor for the stability of charged NMs is ionic strength and the nature of the ions. Brunelli *et al.*[84] used deionized water (DW) as a reference medium to study the stability of P25 NPs. In this way, the presence of any ion that could interact with TiNPs and affect their stability was avoided.[98] It was shown that P25 TiNPs have good colloidal stability. However, the stability of TiNPs was lower in artificial freshwater (AFW) and artificial marine water (AMW), as evidenced by the increase in hydrodynamic diameter and sedimentation velocity. Additionally, a decrease in the absolute value of the zeta potential of the TiNPs was observed in the order DW > AFM > AMW. Generally, it is expected that divalent cations will have a more profound influence on TiNMs' stability than monovalent cations. French *et al.*[43] have shown that at ionic strength and pH values typical for surface waters and soils, it can be expected that the TiNPs aggregates are formed. The higher tendency of TiNPs to aggregate in the presence of divalent Ca^{2+} ion, as compared to Na^+ ion, was ascribed to a higher decrease of Debye length consequently lower electrostatic repulsion potential.

In addition to the properties of the media, the various properties of NMs, such as size, morphology, composition and structure, can significantly impact the stability of suspensions. Marucco *et al.*[91] investigated the stability of TiNPs suspensions without the use of a dispersant. They used TiNPs with diameters of 5 nm and 20–300 nm. Both suspensions exhibited polydispersity and a wide range of particle sizes, as well as very low stability, as sedimentation occurred within 1–2 hours. Liu *et al.*[90] investigated the stability of suspensions of four different types of TiNPs, three types of anatase nanoparticles with nominal diameters of 5, 10, and 50 nm, and rutile nanoparticles with dimensions 10 × 40 nm and 30 × 40 nm. Suspensions were prepared *via* sonication for 2 h, without any dispersant, in DI water and in 5 mM NaCl solution. The results showed that 50 nm anatase and 10 × 40 rutile are the most stable ones, as they almost do not sediment in water and have a slower sedimentation rate in NaCl solution, compared to other samples. 5 nm anatase TiNPs suspension showed slow sedimentation in water, but rather fast in NaCl solution, where it sedimented completely within first few days, while 10 nm anatase TiNPs suspension sedimented quickly in both mediums. The main factor determining the stability of TiNPs aqueous suspensions was shown to be the surface charge, influenced by the varying concentrations of impurities in the pristine material, as the most stable sample had the highest zeta potential values.[90] Degabriel *et al.*[88] have shown, using real-time DLS profiles, that the critical coagulation concentration (CCC) was significantly lower for the rods compared to the spheroids in both NaCl and $CaCl_2$ suspensions. The aggregation was also pH dependent for both spheroids and rods. Doping TiNPs with Er and Yb, can significantly improve TiNPs stability. Although, it was shown that doping of TiNPs did not affect their crystalline structure, suspensions in water and other solvents maintained stability for at least 21 days.[93] Additionally, Sentis *et al.*[95] investigated the dispersibility and stability of suspensions of two TiNPs types, commercial NM-104 and food-grade commercial E171. It was shown that NM-104 had a smaller average primary diameter compared to E171, but was less dispersible, *i.e.*, formed larger aggregates under the same preparation conditions. Nevertheless, it was demonstrated that NM-104 exhibited better stability, characterized by a lower settling velocity and smaller Stokes diameter of aggregates. They also reported the influence of pH on the zeta potential of TiNPs. Results showed that TiNPs E171 had zeta potential around zero at pH = 2, which decreased to −70 mV when pH reached 12. Zeta potential of TiNPs NM-104 had positive values at pH < 6.5, and negative values at pH > 6.5, where in both cases the absolute value of TiNPs zeta potential was around 20 mV.

The method of preparing the suspensions can also significantly influence their stability. The influence of sonication time on suspensions with different TiNPs concentrations and without dispersant was also investigated.[41] It was determined that with an increase in the concentration of TiNPs, the electrophoretic mobility of nanoparticles increased, and their size decreased. Furthermore, it was shown that 20 min sonication is sufficient to disperse agglomerates of TiNPs, while further increases in sonication time had no influence on TiNPs diameter. Phromma *et al.*[94] also investigated the influence of

sonication time and amplitude on the stability of TiNPs suspensions with different concentrations. The authors found that the irradiation of larger amplitude (35%) and duration (15–30 min) was more suitable for lower TiNPs concentrations (0.1 and 1%), while short irradiation (70–140 s) with lower sonication amplitude (20%) was preferable for higher TiNPs concentrations (5 and 10%). By applying these conditions, authors obtained 90 min stability of pristine TiNPs suspensions. Mahbubul *et al.*[39] investigated the influence of sonication duration on particle diameter in TiO_2 suspensions. It was found that the decrease in diameter size with sonication duration had an irregular trend. During the first 30 min of sonication, the value of diameter decreased rapidly. Subsequently, a slight decrease was detected from 30 minutes to 90 minutes. Finally, no

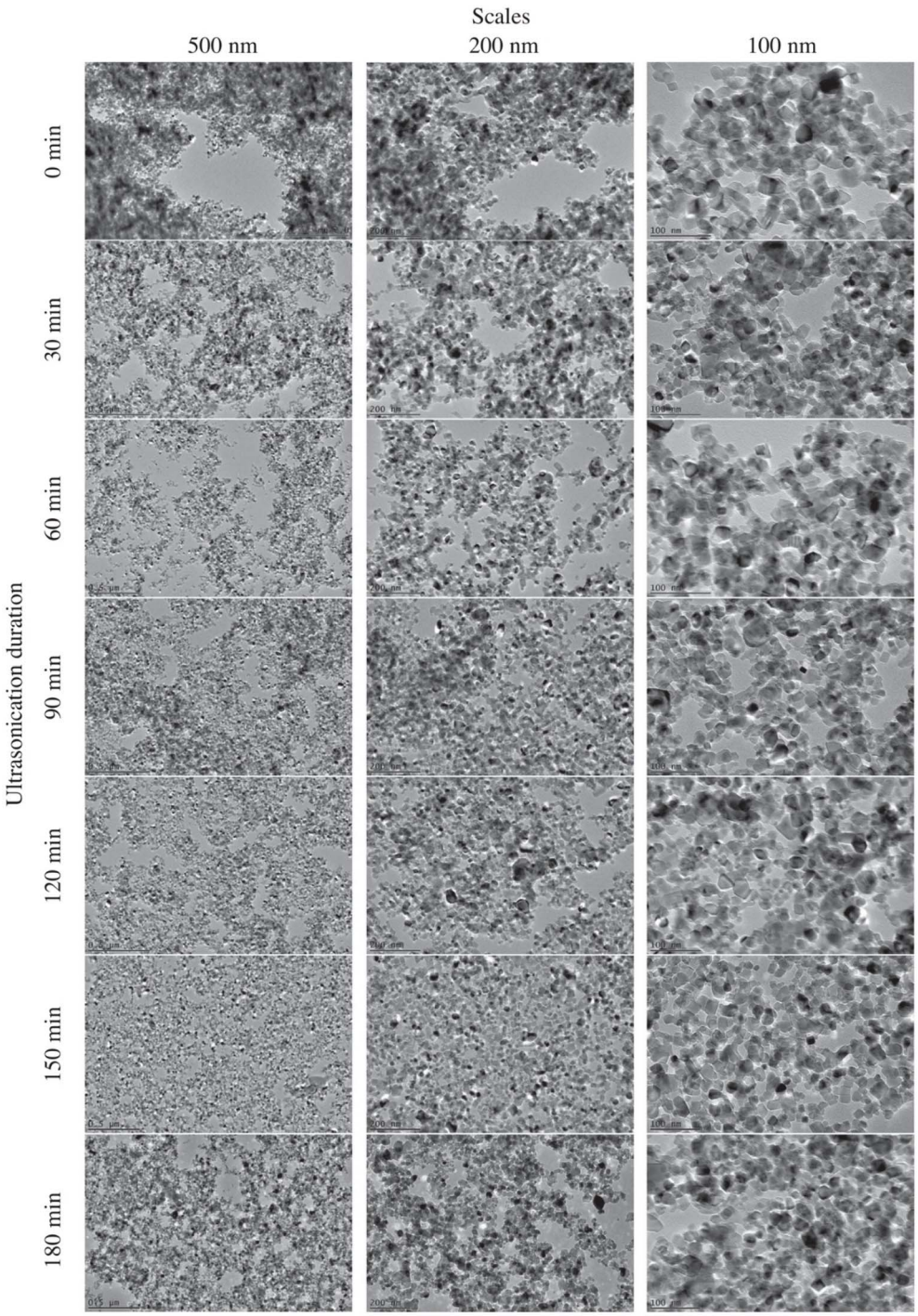

Fig. 4 TEM images of TiO_2 nanoparticles dispersed in water for different periods of ultrasonic treatment. Reprinted from ref. 39 with permission from Elsevier Ltd.

changes in diameter value were observed after the sonification of the sample for 90 min to 180 min (Fig. 4).

Another approach to obtain a stable NMs suspension is to prepare functionalized NMs. This approach is not as frequently used for TiNMs, as for other NMs, like silver nanoparticles.[99] Sen *et al.*[92] studied a novel approach to formulating nanofluids with high solid nanoparticle loading, excellent colloidal stability, low viscosity, and good electrochemical response from the modified nanoparticles. They used sulfonated TiNPs for the preparation of suspensions with solid concentrations up to 50%, demonstrating that surface treatment minimizes particle agglomeration in the presence of electrolytes at pH 11.

The studies reviewed in this section indicate that the stability of pristine TiNMs suspensions is a result of the delicate interplay of several factors, including the properties of TiNMs (structure, size, morphology) and the dispersion media (pH, ionic strength, TiNMs concentration), as well as the type and parameters of the dispersion method. In addition, they also point out that achieving the long-term stability of pristine TiNMs is challenging. However, modifying the surface of TiNMs can facilitate the preparation of stable suspensions. This can be achieved either by doping TiNMs,[93] chemically modifying the surface,[92] or, as described in the following sections, applying different types of dispersants.

4.2. Surfactants

Surfactants (surface active agents, SAA) are amphiphilic compounds that contain a hydrophilic head and a hydrophobic tail in their molecule.[100] Due to their amphiphilic nature, surfactants tend to adsorb at different interfaces at low concentrations, significantly changing the free energy of the surfaces. When all interfaces are occupied, SAA self-assemble in the bulk of the solution into supramolecular structures such as micelles, vesicles, and liquid crystals.[101] Usually, SAA are classified by type of hydrophilic group into anionic, cationic, nonionic, and zwitterionic (Fig. 5).[101] Due to the emergence of SAA with various molecular structures over the past few decades, classification based on molecular structure is becoming increasingly used. Based on the molecular structure, SAA can be classified as single-tail, double-tail, triple-tail, catanionic (two oppositely charged SAA electrostatically bonded), dimeric (two single-tail molecules connected at the level of headgroups by polar or non-polar spacer) and bolaform (two polar groups connected with hydrocarbon chain).[102]

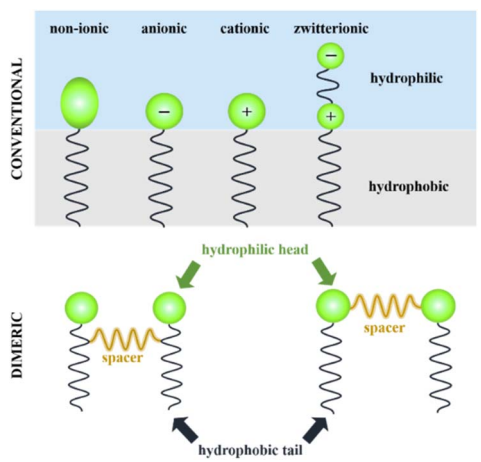

Fig. 5 Schematic representation of the different types of surfactants.

Due to their tendency to adsorb, surfactants are frequently used as dispersants for various nanomaterials.[103] SAA can provide all three mechanisms of stabilization described above. When discussing surfactants' stabilizing effects, it should be considered that in addition to electrostatic and steric interactions, in the case of surfactants, hydrophobic interactions have an important role. This interplay of different forces dictates their adsorption behaviour at solid surfaces. The difference in the adsorption behaviour of ionic surfactants, as compared to other charged adsorbates, is depicted in the adsorption isotherm. Ionic surfactant adsorption isotherm usually exhibits four regions.[104] At low surfactant concentrations, surfactant molecules adsorb at the oppositely charged solid surface. Upon increasing surfactant concentration, lateral interactions between hydrophobic chains become important, and surfactant molecules form surface aggregates, like hemi-micelles, admicelles, *etc.* As a result, adsorption density increases sharply in this region. When the amount of adsorbed surfactant molecules is high enough to electrically neutralize a solid surface, further adsorption proceeds through lateral attraction only. At concentrations above the critical micellization concentration (cmc), further increase in surfactant concentration leads only to micellization in the solution, while the adsorption density remains unchanged. Hydrophobic interactions govern the adsorption, surfactant molecules adsorb in a reversed orientation, with head groups oriented towards the bulk of the solution.[104] This section provides an overview of the most commonly used surfactants for stabilizing TiNMs (Table 2).

Sodium dodecyl sulphate (SDS) is a frequently used model anionic surfactant. Several studies have investigated its efficiency in stabilizing TiNMs suspensions, as well as compared its influence with that of other surfactants. Yang *et al.*[34] investigated the effect of varying SDS concentrations on the stability of TiNPs suspensions in both water and 100 mM NaCl. It was shown that the stability of suspensions increases with SDS concentration up to the cmc. A further increase in SDS concentration led to the instability of suspensions due to the formation of micelles, as strong depletion forces prevailed. The stabilizing effect of SDS was compared with the effect of cationic cetyltrimethylammonium bromide (CTAB), dodecyltrimethylammonium bromide (DTAB), benzethonium chloride, tetradecylpyridine bromide (TDPB) and dimeric bis(*N*,*N*-dimethyl-*N*-dodecyl)ethylene-1,2-diammonium dibromide (12-2-12) and bis(*N*,*N*- dimethyl-*N*-dodecyl)hexane-1,2-diammonium dibromide (12-6-12), anionic sodium dodecyl benzene sulfonate (SDBS), nonionic triblock copolymer Pluronic F-127, nonylphenol ethoxylate (NPEO) and Triton X100. Cationic SDS and CTAB were shown to be more efficient in stabilizing TiNPs nanofluids compared to anionic SDBS and acetic acid. However, CTAB was preferred for the preparation of nanofluids with high particle loading (>1%),[105] confirming a previous study showing that CTAB can be used for adequate stabilization of

Table 2 Summary of the reviewed studies investigating the stability of aqueous suspensions of TiO_2 nanomaterials (TiNMs) in the presence of surfactants as dispersants

Dispersant[a] (concentration in solution)	TiNMs (w/v concentration in suspension)	Homogenization method	Ionic strength	pH	Reference
SDS (0.1–200 mM)	Nanoparticles, rutile, TR52 (1%)	Stirring, 30 min Sonication, 3 h	100 mM NaCl	—	34
CTAB, SDBS, SDS (0.1%, 0.5%, 1%)	Nanoparticles, anatase (0.1–1%)	Sonication, 15 min	—	—	105
CTAB, SDS (0.2–20%)	Nanoparticles, anatase (0.1–2%)	Agitation, 2 h	—	3–5	106
SDS, CTAB, Pluronic F-127 (1–3%)	Nanoparticles, anatase (0.05%)	Sonication, 30 + 30 min	—	—	107
SDS (0–4 mM), TDPB (0–2.5 mM), TX100 (0–4 mM)	Nanoparticles, rutile (20%)	Sonication, 2 min	50 mM NaCl	—	108
SDS, NPEO (0–0.03%)	Nanoparticles, anatase (0.005%)	Shaker, 140 rpm	—	—	109
BTC, SDBS, TX100 (0–2.87 M)	Nanoparticles, rutile (0.1–0.2%)	Stirring, 2 h	—	2–12	110
POE-DETADAA (20% w/w)	Nanoparticles, rutile	Shaker, 20 min	—	—	111
12-6-12 (1 and 250 × 10^{-6} M), SDS (5 × 10^{-3} M)	Nanoparticles, P25 (0.05–0.5%)	Sonication, 1 h	5 mM KBr	4.5	112
12-6-12 (1 and 250 × 10^{-6} M)	Nanoparticles, P25 (0.1%)	Sonication, 1 h	5 mM KBr	—	113
DTAB (0.1 M), 12-2-12 (0.01 M)	Nanowires TiO_2(B) and trititanate (mixed), (0.001–0.01%)	Sonication, 30 min	0 or 1 mM NaBr	—	114

[a] BTC – benzethonium chloride, CTAB – cetyltrimethylammonium bromide, DTAB – dodecyltrimethylammonium bromide, NPEO – nonylphenol ethoxylate, POE-DETADAA – polyoxyethylene diethylenetriamine dialkylamide, SDS – sodium dodecyl sulphate, SDBS – sodium dodecyl benzene sulfonate, TDPB – tetradecylpyridine bromide, TX100 – Triton X100, 12-2-12 – bis(*N*,*N*-dimethyl-*N*-dodecyl)ethylene-1,2-diammonium dibromide, 12-6-12 – bis(*N*,*N*-dimethyl-*N*-dodecyl)hexane-1,2-diammonium dibromide.

anatase TiNPs nanofluids.[106] It was shown that both cationic SDS and CTAB, as well as non-ionic Pluronic F-127 have a similar effect on the stability of TiNPs suspensions, maintaining the suspensions stable for 1 h. However, the influence on particle size differed, as the smallest particles were observed in the presence of CTAB.[107] Chen *et al.*[108] compared the efficacy of SDS, cationic TPB, and non-ionic Triton X-100 in providing stabilization for TiNPs dispersions. It was found that SDS and TPB, as ionic surfactants, enhance the stability of dispersions, while non-ionic TX 100 has a negligible influence on TiNPs suspension stability. Contrarily, Li *et al.*[109] have shown that both SDS and non-ionic NPEO are efficient in preventing aggregation in MilliQ water and water from different environmental sources. However, anionic SDS was more efficient. The study was designed and performed in a batch experiment conducted in a shaker to better simulate the dynamics of the natural water environment.

These studies do not report the pH at which they were performed, which could correlate the observed effects with the zeta potential of TiNMs in the media. This void, however, is filled by study of Petryshyn *et al.*[110] They studied the effect of cationic benzethonium chloride, anionic SDBS, and non-ionic TX-100 on the aggregation behaviour of rutile TiNPs with a size of 230 nm in a wide pH range of 2–12. All surfactants improved TiNPs stability. At pH > pH_{IEP} for anionic surfactant, and at pH < pH_{IEP} for cationic surfactants, high aggregation stability was observed. At pH < pH_{IEP} for anionic surfactant and at pH > pH_{IEP} for cationic surfactant, stability increased with surfactant concentration.

Sato and Kohnosu[111] showed non-linear dependence of rutile TiNPs (210 nm in size) stability with increasing polyoxyethylene diethylenetriamine dialkylamide concentration. At low surfactant concentrations, stability initially decreases, accompanied by the zeta potential becoming less negative. Minimum stability was observed at the surfactant concentration for which the zeta potential was 0 mV. A further increase in surfactant concentration resulted in a more positive zeta potential, accompanied by an increase in stability. Maximum stability was observed at the surfactant concentration at which a plateau in adsorption was reached. Further increase in surfactant concentration resulted in destabilization. This behaviour was attributed to the reduction of electrostatic repulsion at lower surfactant concentrations and the depletion effect at higher concentrations, as evidenced by the absence of changes in adsorption and zeta potential.

Dimeric surfactants have been attracting attention due to their superior properties compared to their conventional counterparts.[115] This makes them of high interest in both fundamental research and industrial applications. Veronovski *et al.*[112] studied the stabilization properties of 12-6-12 and SDS, and reported that at all investigated concentrations, dimeric surfactant showed better stabilization properties, indicated by the mean particle size of TiNPs in suspension. In the following study,[113] authors observed that upon the increase in 12-6-12 concentration, an increase in pH and sedimentation occurred. As the zeta-potential value approached 0 mV, it was concluded that a monolayer of 12-6-12 molecules was formed with hydrophobic tails protruding from the surface of TiNPs, inducing

aggregation. With increasing 12-6-12 concentration up to cmc, the stability increased, which was ascribed to the formation of a bilayer on the surface of TiNPs with charged head groups oriented outside. Selmani *et al.*[114] compared the influence of two structurally different quaternary ammonium surfactants, monomeric DTAB and the corresponding dimeric 12-2-12, on the stability of TiNWs in water and aqueous NaBr solution. It was shown that aqueous suspensions of TiNWs are rather stable but that the addition of NaBr induces aggregation, which becomes more pronounced with the increase of TiNWs concentration. 12-2-12 acted as a stronger stabilizer than DTAB, due to the presence of two positively charged head groups and two hydrophobic tails. The results were theoretically confirmed by the surface complexation model (SCM). SCM showed that 12-2-12 had a higher intrinsic log K, thus confirming that 12-2-12 interacts more strongly with TiNWs surfaces compared to DTAB. The reason for this behaviour may be the different structure of adsorbed surfactant layers, which is a consequence of their different molecular structures. The model was able to predict zeta potential values as a function of pH, TiNWs concentration, salt level, and surfactant concentration, providing a way to tailor the stability of TiNWs dispersions and enabling a better understanding of the surfactant behaviour in contact with TiNWs surfaces.

In summary, the surfactants were demonstrated to be efficient dispersants under various conditions. Applying surfactants of different molecular structures can enable fine-tuning the stability of suspensions by utilizing electrostatic, steric, and hydrophobic forces. This makes them of special interest for various applications. Despite the above-mentioned advantages, studies have shown that another class of dispersants, namely polymers, can be more efficient than surfactants.

4.3. Polymers

Polymeric dispersants differ from inorganic or small organic molecules due to their relatively higher molecular weights, which often enable achieving higher colloidal stability of nanomaterials.[116] A polymeric dispersant containing functional anchoring groups attached to the backbone chain can bind to the numerous sites on the titania surface and form adsorption layer(s) or extend from the surface of the nanomaterials to the bulk solution. The dispersion role of such macromolecules depends on the thickness and durability of the adsorbed polymer layer. The most common polymeric functional groups are carboxylic, sulphonic, and phosphoric acid groups, phosphate esters, amines, ammonium, and quaternary ammonium groups.[117] Depending on the charge of the associated functional groups, polymeric dispersants can be divided into two classes: (i) ionic (which provide electrostatic stabilization) and (ii) non-ionic (which provide steric stabilization). Ionic functional groups make polymeric dispersants effective in the aqueous phase, where the stabilization performance depends on pH value and ionic strength. On the other hand, non-ionic dispersants are generally not sensitive to solution chemistry and are, therefore, also an effective stabilizer in the dry state (*e.g.*, in drying processes of TiNMs-based coatings or during the extraction of nanomaterials from a liquid phase). In both cases, for achieving stable suspensions, the careful selection of an optimal polymer concentration is crucial. An excess amount of polymer can result in increased viscosity or unintended interactions, while a low concentration may not be effective enough. In Table 3, a summary of the studies on the influence of polymeric dispersants on the stability of TiNMs suspensions is provided. As it can be seen, the majority of the polymers listed below are, in fact, ionic, which indicates that they stabilize suspensions through an electrostatic stabilization mechanism.

The molecular weight of the polymer is important factor in determining its efficacy to stabilize NMs suspensions. Therefore, it is not surprising that a number of studies investigated the relationship between molecular weight and efficacy of polymer to stabilize TiNMs suspensions. Polyacrylic acid (PAA) is the most commonly used polymer for stabilizing TiO_2 suspensions. Sato *et al.*[118] showed that the aggregate size of the ultrasonically treated TiNPs suspension with sodium polyacrylate (NaPAA) was close to the primary particle size estimated from the specific surface area in relatively concentrated suspensions with a solid fraction of up to 15 vol%. The optimum molecular weights of NaPAA for nanoparticle dispersion by ultrasonication were 8000 or 15 000 g mol^{-1}. Othman *et al.*[40] investigated the influence of PAA molecular weight on dispersing and stabilizing TiNPs, produced using the metal organic chemical vapour deposition method, in aqueous suspensions. The use of ultrasonication was found to assist the agglomerates to break down into smaller agglomerates and aggregates, confirming previous observations.[118] Moreover, the addition of dispersant was found to improve the deagglomeration process *via* ultrasonication by enhancing the separation between nanoparticles and hindering the agglomeration of the nanoparticles. The low-molecular-weight dispersant, PAA 2000, produced a more stable suspension with smaller average cluster size than obtained in the presence of PAA 5000. The reason is most likely the fact that polymers of high molecular weight have longer carbon chains that can bridge many nanoparticles, resulting in a larger average cluster size. The optimum amount of dispersant to disperse and stabilize the TiNPs aqueous suspensions was found to be 3 wt%. Also, the suspension stabilized with PAA 2000 remained stable for more than 2 months.[40] Sun *et al.*[119] also investigated the influence of PAA molecular weight (M_w = 100 000, 450 000 and 1 250 000). Contrary to the general opinion that high M_w polymers would exhibit better flocculation performance, their study found that medium M_w PAA performed the best, in line with results obtained by Othman *et al.*[40] In addition, although the settling rates differed for different M_w PAA, all polymers exhibited optimal flocculation performance at 3.3% of a monolayer coverage of TiNPs surface. As the efficient adsorption of the dispersant on the surface of NMs is crucial for obtaining stable suspensions, the adsorption behaviour of PAA at the surface of dispersed titanium dioxide was also investigated at different concentrations, pH levels, and PAA molecular weights.[120] Adsorption isotherms indicate that the adsorption density of PAA increases at low concentrations of PAA and then reaches a saturation value at higher concentrations, as expected. The adsorption

Table 3 Summary of the reviewed studies investigating the stability of aqueous suspensions of TiO_2 nanomaterials (TiNMs) in the presence of polymers as dispersants

Dispersant[a] (concentration in solution)	TiNMs (w/v concentration in suspension)	Homogenization method	Ionic strength	pH	Reference
NaPAA (0.5 mg per m^2 of TiNPs surface)	Nanoparticles, P25 – anatase/rutile and ST21 – anatase (1%; 15%)	Sonication, 30 min Ball milling, 60 rpm, 24 h Bead miling, 3 h	—	8.5	118
PAA, Darvan C (0–3%)	Nanoparticles, anatase (0.05%)	Sonication	—	8.5	40
PAA (0.1%)	Nanoparticles (1%)	Stirring, 24 h	—	3	119
PAA (0.00 1%; 0.01%)	Nanoparticles, anatase (2%)	Sonication and stirring, 30 min	—	2.5–9.5	120
Duramax D-3005 (PAA salt)	Nanoparticles – anatase, rutile	Sonication, 0–5 min, orbital shaker 30 min	—	—	121
NH_4PAA (10% based on TiNPs mass)	Nanoparticles, R-706 – rutile; P90 and NKT 90 – anatase/rutile (5%)	Mixing, 100 rpm, 1 h	—	8	122
NaPAA (0.02% and 0.5%)	Zirconia- and alumina-coated nanoparticles (20–60%)	—	—	3–9.5	123
PAA, PBTCA, CEPA (0.4%)	Nanoparticles, rutile (2.5%)	Stirring, overnight	0.01 M KCl	5.5; 9.5	124
PAA (1–7 wt%)	Nanoparticles, P25 (0.05–0.005 wt%)	Stirring, 24 h	—	—	125
PAA, PMA, PEA (monomer 0.1 mM)	Nanoparticles (0.1%)	— High-power ultrasound probe	—	—	35
PEG-*b*-P4VP, NaPAA	Nanoparticles, P25 (1 wt%)	Rotor-stator high-shear mixer Cowles-type disperser, 2000 rpm	—	9	36
PEG, SN5040 (1–5%)	Nanoparticles, P25	Stirring, several hours	—	2–12	126
PEG, PVP	SRM NIST 1898 reference material (0.01–0.3%)	Ultrasonic bath (60 min) Ultrasonic horn (pulse mode, 2–10 min)	—	—	127
POEOA (0.1%)	Nanoparticles, Al_2O_3 dopped (0.01%)	Sonication	—	9, 5	128
Darvan C (0.01–0.14%)	Nanoparticles, anatase/rutile (1%)	Equilibration, 24 h	—	3; 6; 9	129
P4VP, PAH, PAA (10^{-4} M)	Nanoparticles, anatase Rectangular, rutile (0.01%)	Ultrasonic bath (15 min) + ultrasonic probe (15 min) + magnetic stirring (1300–1500 rpm)	0.01 M NaCl 0.1 M NaCl	3; 4; 7 and 11	130
Mixture of PAAH and PVA (38–50% of dry mass)	Nanoparticles (2–12%)	Shaking 2500 rpm 10 min sonication 30 min	0.1 M NaCl 0.1 M KCl	2–12	131

[a] CEPA – 2-carboxyethylphosphonic acid, Darvan C – ammonium salt of polymethacrylic acid, NaPAA – sodium polyacrylate, NH_4PAA – ammonium polyacrylate, PAA – polyacrylic acid, PBCTA – phohosphonobutane tricarboxy acid, PDMAEMA – poly(2-(dimethylamino)ethyl methacrylate, PAH – polyallylamine hydrochloride PEA – polyethacrylic acid, PEG – polyethylene glycol, PEG-*b*-P4VP – poly(ethyleneglycol)-*b*-poly(4-vinyl pyridine) block copolymer, PMA – polymethacrylic acid, POEOA – poly[oligo(ethylene oxide)methyl ether acrylate], PVA – polyvinyl alcohol, PVP – polyvinylpyrrolidone, P4VP – poly(*N*-ethyl-4-vinylpyridinium) cation, SN5040 – commercial dispersant NaPAA.

density of PAA is found to increase with an increase in PAA molecular weight. The increase in pH of the solution results in a decrease in the adsorption density of PAA. The determined thickness of the adsorption layers of PAA on the titanium dioxide surface increases with increasing pH, as well as with increasing polymer concentration and molecular weight.

Different effects were observed when comparing stability of suspensions containing different TiNPs depending on their structure and surface properties. Fazio *et al.*[121] investigated the stabilization effect of the commercial salt of a polyacrylic acid-based polyelectrolyte, DURAMAXTM D-3005, on suspensions of three different TiNPs, namely commercial anatase, commercial rutile, and anatase synthesized by the cryo-gel technique. Stable suspensions of commercial TiNPs were obtained at 1.0–1.5 wt% of polyelectrolyte. However, it was not possible to obtain a stable suspension of synthesized TiNPs. Tsai *et al.*[122] investigated the stabilization effect of ammonium polyacrylate (NH_4PAA) on hydrophilic and hydrophobic nano-sized TiO_2, both being mixture of anatase and rutile. Different surface chemistry resulted in different affinity towards NH_4PAA. Better stabilization was observed for hydrophilic TiNPs, even though a thicker NH_4PAA layer was formed on hydrophobic TiNPs. Thermodynamic calculations showed that steric stabilization dominated the dispersion of hydrophilic TiNPs. Karakaş and Çelik[123] used zirconia- and alumina-coated TiNPs and investigated the effect of NaPAA on the stability of their suspensions. They demonstrated that stabilization is achieved in the plateau concentration region of the adsorption isotherm, where values of the zeta potential have a large absolute value (Fig. 6). It was concluded that the electrosteric mechanism governs stabilization. Aggregation of pristine and different polyelectrolyte-coated TiNPs (0.01%) was investigated under different pH and IS.[130] Pristine TiO_2 particles tend to aggregate very fast in the isoelectric region (pH around 6.5). Outside of this region, colloidal stability can be achieved depending by the IS of the base electrolyte. However, when TiO_2 particles are stabilized with polyions, either with strongly charged poly(*N*-ethyl-4-vinylpyridinium cation (P4VP), weakly charged poly(-allylammonium) cation (PAH) or weakly charged PAA, negligible particle clusters are formed. An increment in IS generally results in the weakening of electrostatic interactions between the individual particles, *i.e.* to the formation of the aggregates. The degree of polyanion ionization plays an important role in $TiNPs_2$ stabilization; for example, the aggregation rate of PAA-coated particles was found to be 0.9 nm s^{-1} at pH = 3, since PAA ionization was less than 5%.

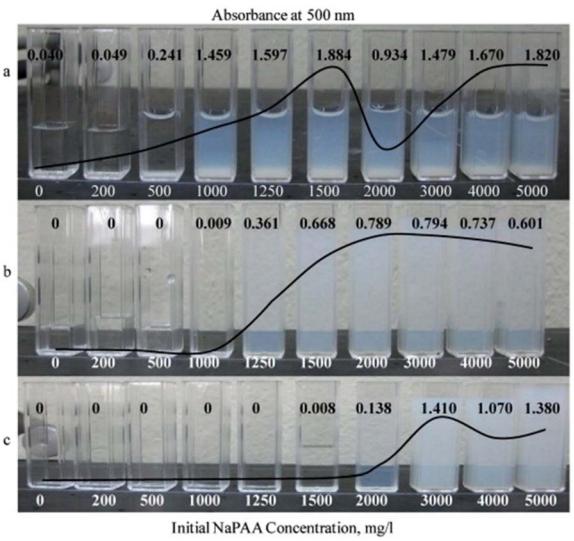

Fig. 6 Settling behaviour of TiO_2 suspensions after 50 days of aging at different initial NaPAA concentrations: (a) 20 wt%, (b) 30 wt%, (c) 40 wt%. Reproduced from ref. 123 with permission from Elsevier Ltd.

A number of studies compared the stabilization efficacy of different polymers and other types of dispersants with that of PAA. Cran *et al.*[124] compared the behaviour of PAA and phosphonates, namely 2-carboxyethylphosphonic acid (CEPA) and phosphonobutane tricarboxy acid (PBCTA). They suggested that PAA and CEPA provide electrostatic stabilization to pigment particle suspension, whereas grafted PBCTA provides both electrostatic and steric stabilization. Elbasuney *et al.*[117] employed PAA and dodecenylsuccinic anhydride (DDSA) for post-synthesis surface modification of TiNPs to improve their dispersibility by altering surface properties. The authors obtained effectively stabilized TiNPs coated with PAA in aqueous media, and TiNPs coated with DDSA stabilized in organic media. Tsai *et al.*[125] compared the PAA stabilizing properties with ones of small molecular anionic sodium hexametaphosphate (SHMP). It was found that 5% of both stabilizers was sufficient for the stabilization of TiNPs dispersions. Berglez *et al.*[35] investigated different poly(α-alkyl carboxylic acids) (PAA, polymethacrylic acid, PMA, and polyethacrylic acid, PEA) to determine the influence of chain length and stereochemistry on the stability of TiNPs. The addition of the most hydrophilic PAA to TiNPs suspension resulted in the largest shift of pH_{IEP} and the best stabilizing effect among tested dispersants. It was demonstrated that stereochemistry has a lesser influence on the stability of TiNPs suspensions. Monteiro *et al.*[36] synthetized novel poly(ethyleneglycol)-*b*-poly(4-vinyl pyridine) block copolymer (PEG-*b*-P4VP) and tested it against NaPAA for stabilization of 1% TiNPs dispersion at pH = 9. The obtained results suggested that PAA was superior in preventing aggregation. However, block copolymers showed better particle size distributions and dispersion stability over time. Peng *et al.*[126] investigated the influence of PEG and SN5040, individually and in a mixture, on the stability of P25 TiNPs aqueous suspensions with the aim of preparing inner wall latex paint. SN5040, a commercial dispersant whose main component is NaPAA, proved to be a more efficient dispersant in basic conditions. The addition of a simple electrolyte, NaCl, resulted in an increase in the optimal SN5040 concentration. Interesting effects were observed when SN5040 and PEG were applied in a mixture. If the polymers were added simultaneously, an antagonistic effect was observed. However, when added sequentially, a synergistic effect was observed, ascribed to reduced electrostatic repulsion between SN5040 molecules due to the presence of PEG. The screening of electrostatic interactions enabled an increase in SN5040 adsorption density. The suspension was successfully

applied in the preparation of the paint. In another study, PEG and PVP were used as polymeric dispersants to prepare a stable TiNPs dispersions in aqueous and biological samples.[127] Optimization of the various parameters (type of polymeric stabilizer, mode of dispersion, dispersion type) was performed using SRM NIST 1898 NP reference material, which includes anatase and rutile crystal forms. The results revealed that the addition of PVP polymer at 2 wt% concentration and sonication of the suspension with a probe (2 min at 80% pulse mode) hinders the formation of a larger agglomerate for at least 72 h. Another group of authors also reported the preparation of stable suspensions using PVP as dispersant, where the optimal concentration was found to be 0.04 times the concentration of TiNPs.[94]

Ammonium salt of polymethacrylic acid (Darvan C) was another polymer studied for stabilization of TiNP, and it was indicated that the stability of suspensions increased with Darvan C concentration, although stability was lower than in the presence of PAA 2000.[40] Investigations of Darvan C adsorption on TiNPs revealed that the adsorption of Darvan C results in a significant shift of pH_{IEP} towards lower pH values. Adsorption isotherms were of Langmuir type, and results indicated that the adsorption occurs through electrostatic interactions, in addition to hydrophobic.[129]

Deshmukh *et al.*[131] investigated the stability of TiNPs suspensions in the mixture of polyallylamine hydrochloride and polyvinyl alcohol under a wide range of pH (2–12), TiNPs content (2–12%), and temperatures (25–65 °C). As no sedimentation was observed in the course of 2 months, it was concluded that the suspensions were rather stable.

Tailor-made dispersants attract special attention in the development of stable suspensions. However, the studies of tailor-made polymeric dispersants for TiNMs are scarce. Rezende *et al.*[128] synthesized tailor-made dispersants poly[oligo(ethylene oxide)methyl ether acrylate] (POEOA) as hydrophilic block and poly(2-(dimethylamino)ethyl methacrylate) (PDMAEMA) and dopamine (Dopa) as anchoring molecules by atom transfer radical polymerization. They validated their TiNPs stabilizing performance using satin vinyl paint. A better TiNPs suspension was observed compared to conventional PAA.

In summary, polymers, due to their high molecular weight, enable efficient stabilization of TiNMs. Their two principal mechanisms of action are electrosteric and steric stabilization. Electrosteric stabilization can be successfully achieved by applying weak or strong polyelectrolytes.[130] Steric stabilization is provided using non-ionic polymer chains, such as PEG[126] and PVP.[127] For both stabilizing mechanisms, the good surface coverage of TiNMs with polymer is crucial. The importance of the polymeric M_w must be emphasized here. It was shown that better colloidal stability can be achieved with polymeric chains of lower M_w, since longer chains could intertwine or create bridges between the adjacent particles, forming larger aggregates.[40,119] Although it is usually thought that polymers are more efficient than small molecules, there is proof that, in some cases, small molecules can be as efficient at the same concentrations.[125] Therefore, the effectiveness of the small organic and inorganic molecules is discussed in the next section of the manuscript.

4.4. Small organic and inorganic molecules

Recent investigations in the effects of small molecules on the stability of TiNMs suspensions highlight their role in facilitating the stabilization, *i.e.*, agglomeration suppression in TiNMs.[132] The reviewed studies dealing with small molecular dispersants are summarized in Table 4.

Among the inorganic species used for the encapsulation of TiNMs, various phosphates were the most dominant. Due to the multiple oxygen donor atoms, *i.e.* three pK_a values, phosphates can adsorb to the surface of nanomaterials from either acidic or basic solutions, making them an excellent functional moiety to stabilize TiNMs.[133]

In the work by Kao and Cheng,[38] sodium hexametaphosphate (SHMP) was employed as the dispersant. Based on visual observation, the results indicated that 0.1 wt% suspension of TiNPs stabilized with 0.2 wt%. SHMP could be stable for approximately two weeks. The strong adsorption of phosphate has resulted in a strongly negative charged surface, with a measured zeta potential of −53.7 mV. Additionally, they have determined that SHMP contributed to the reduction in secondary particle size using DLS (Fig. 7). The phosphate dispersant adsorbed onto TiNMs surface prevented its precipitation, even at near-supercritical CO_2 conditions.

Tsai and co-workers[125] demonstrated that stable TiNPs suspensions can be obtained at 5 wt% of both inorganic (SHMP) and organic (PAA) dispersants. The good efficacy of SHMP was ascribed to the higher electronegativity and stronger electrostatic repulsive forces. In another study, the dispersing efficiency of SHMP was also investigated, together with ethanol, tetrahydrofuran (THF), and polyvinylpyrrolidone (PVP).[134] The results revealed that the stability of suspension strongly depends on the concentration of the dispersant, as 2 vol% of THF and 0.02 g per mL SHFM were most efficient for stabilizing suspension containing 0.1% TiNPs. Sodium tripolyphosphate (STPP), another inorganic phosphate species, has been successfully employed to disperse anatase nanoparticles in water.[135] A stable suspension of 30 wt% TiNPs with smaller particle clusters (average diameter ~30 nm) was subjected to a plasma spraying process as a coating method to fabricate a photocatalytic ultrafiltration membrane on stainless steel substrates.

Specific effects of various inorganic anions, including biphosphate, on the stability of aqueous titania nanosheets (TiNSs) suspensions were investigated in acidic (pH = 4) and basic (pH = 10) conditions.[136] The results revealed that, in acidic media in which they act as counterions, the majority of the monovalent species destabilized the suspensions, according to the Hofmeister series. However, monophosphate/biphosphate exhibits atypical behaviour under acidic ($H_2PO_4^-$ present as a major species) and alkaline (HPO_4^{2-} present as a major species) conditions, rendering unusually low and high critical coagulation IS (CCIS) values, respectively. Namely, the strong affinity of phosphate to coordinate the Ti surface atoms

Table 4 Summary of the reviewed studies investigating the stability of aqueous suspensions of TiO_2 nanomaterials (TiNMs) in the presence of small molecules as dispersants

Dispersant[a] (concentration in solution)	TiNMs (w/v concentration in suspension)	Homogenization method	Ionic strength	pH	Reference
SHMP (0.0025–0.025%)	Nanoparticles, P25 (0.005–0.1 wt%)	Stirring (950 rpm, 24 h); $SCCO_2$	—	2.0–12.0	38
SHMP, PAA (1–7 wt%)	Nanoparticles, P25 (0.05–0.005 wt%)	Stirring, 24 h	—	6.2; 7.7	125
SHMP (0.5–2.5%), THF (0.5–3%), ethanol (5–30%) PVP (0.5–2.5%)	Nanoparticles, anatase (0.1%)	Sonication, 30 min	—	—	134
STPP (3 wt%)	Nanoparticles, anatase (20–30 wt%)	Agitation and sonication	—	10.0	135
$H_2PO_4^-$/HPO_4^-	Nanosheets (0.1%)	—	10–1000 mM	4, 10	136
Dopamine, Tiron (0–1.75% based on TiNPs mass)	Nanoparticles, P25 (2%)	Sonication	—	3.0–9.0	137
OA, OLA	Needle-shaped rutile nanopowder (1%)	Ball-milling, 4 h	—	—	138
OA, oleyl phosphate, OLA, tris-(2-butoxyethyl) phosphate (0–60 × 10^{-3} M)	Nanoparticles, R-706 – rutile and NKT90 – rutile/anatase (1%)	Ball-milling, 24 h	(Dispersed in ethyl acetate)	—	33
Glycine, malic acid, malonic acid and glycerol	Anatase (31–45 wt%)	*In situ* stabilization	(Dispersed in benzyl alcohol)	—	37
Azulene (0.00025–0.001%)	Nanoparticles, N-doped, anatase (0.3%)	—	—	—	139
Oxalic and adipic acid (0.1–2.2 mM)	Nanoparticles, anatase (0.05–0.6%)	Mixed on a circular rotator for 2 h	0.02 M NaCl	2.0–6.5	140
SA (0–10 ppm)	Nanoparticles, P25 (166 ppm)	Sonication 45 min at 60 °C, stirring 45 min at 60 °C	—	4.0; 11.0	30
Tiron (0.3 wt%)	Nanoparticles, rutile TRHP2	—	0.01 M NaCl	3.0; 11.0	141
HCl, HNO_3, NH_3, EG (5 wt%)	Nanoparticles, P25 (0.25–1%)	Stirring, 30 + 30 min Sonication, 60 + 5 min	—	2.5–9.5	142

[a] EG – ethylene glycol, OA – oleic acid, OLA – oleylamine, PAA – poly(acrylic acid); SA – salicylic acid, SHMP – sodium hexametaphosphate, STPP – sodium tripolyphosphate.

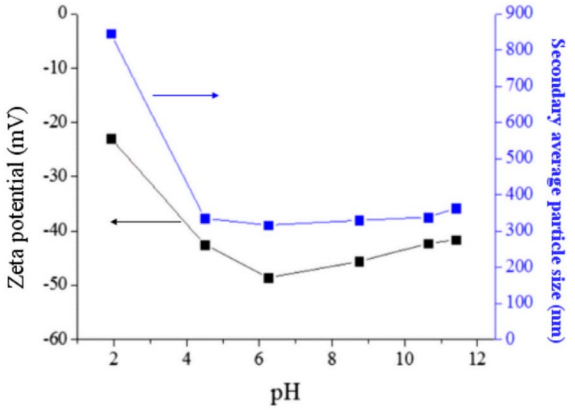

Fig. 7 Zeta potential and the secondary average particle size estimated by DLS in aqueous TiO_2 dispersion (0.005 wt%) containing 0.01 wt% SHMP through supercritical CO_2 (t = 35 °C, p = 1200 psi, saturation time 30 min). Reproduced with permission from ref. 38. Copyright under ACS AuthorChoice Licence.

through two oxygen atoms (bidentate binding mode) resulted in a remarkable charge reversal of TiNSs. Therefore, for both phosphate species, due to their strong interaction with the TiNSs, the presence of forces of non-DLVO origin was determined.

These studies indicate that for the efficacy of inorganic small molecular dispersants, the presence of several functional groups in its structure is of paramount importance, as their primary mode of action is electrostatic repulsion. In addition, polyprotic groups enable application in a wide pH range.

In addition to inorganic molecules, suitable small-molecular-weight organic molecules can also be highly effective dispersants. Sallem *et al.*[137] focused on two catechol derivatives, namely Tiron (disodium 4,5-dihydroxy-1,3-benzendisulfonate) and dopamine (2-(3,4-dihydroxyphenyl) ethylamine). By dissolving Tiron in water, a negatively charged (anion) species is obtained, while dopamine is effectively protonated in a wide range of pH and is thus positively charged in solution. Both Tiron and dopamine not only stabilized the TiNPs suspension in their respective pH ranges but also decreased the viscosity of highly loaded titania suspensions. Thus, an overall increase in the maximum attainable concentration of TiNMs was achieved, albeit under different pH regimes, depending on the chosen dispersant.

Li *et al.*[138] explored the effects of surface modification of TiNMs by treating them with acid or coating them with a few nanometres thick layer of silica (SiO_2). Additionally, they have treated the coated TiNMs with acid. The SiO_2 coated TiO_2 had a significantly lower isoelectric point, making the particle surface acidic. On the other hand, the acid-treated TiO_2, which had its silica layer thinned to less than a nanometre, exhibited similar surface properties to pristine TiNMs. Furthermore, they have investigated oleic acid (OA) and oleylamine (OLA) as dispersants. The acidity of the SiO_2-coated TiO_2 surface favoured OLA adsorption and hindered OA, due to unfavourable electrostatic interactions. The acid-treated TiO_2 favoured the adsorption of OA and OLA to a similar extent. Their findings emphasize the importance of the isoelectric point on the adsorptive interactions between NMs and dispersants in general. Yang *et al.*[33] investigated the suspension performance of three common organic dispersants with carboxyl, amino, or phosphate moieties, namely OA, OLA, tris-(2-butoxyethyl phosphate), for the stabilization of hydrophilic and hydrophobic TiO_2 in ethyl acetate, a polar aprotic solvent. Their results have shown that hydrophilic TiNMs are more sensitive to the choice of dispersant, even though a sufficient level of dispersant adsorption is crucial for achieving stable suspensions. In addition, hydrogen bonding and charge-based interactions, in the case of dispersants with hydroxyl and phosphate functional groups, both play important roles in preventing irreversible agglomeration in polar, aprotic solvents. Suspensions of high solid TiNPs loading (up to 45%) can be obtained with *in situ* encapsulation of particles with small-molecule organic ligands such as glycine, malic acid, malonic acid and glycerol.[37] *In situ* stabilization, in which the stabilizer molecule is present during the formation of NMs, ensures good binding of the ligand and optimum colloidal stability. Regardless of the type of organic molecule used, stabilization of all systems is achieved through strong electrostatic repulsion in highly acidic media (pH around 1). Upon neutralization, precipitation occurs in all suspensions, indicating a negligible effect of these organic stabilizers.

Vaiano and co-authors[139] demonstrated that azulene, a non-benzoid aromatic hydrocarbon, has a significant impact on the statistical distribution of TiNMs populations in aqueous suspensions. Azulene effectively altered the aggregate size distribution of N-doped TiO_2 particles from a trimodal to an essentially monomodal distribution. In addition, azulene as a dispersant enhanced the photocatalytic properties of the titania suspension. By preventing large-scale aggregation, the dispersant ensured enhanced contact between the TiO_2 surface and the methylene blue target pollutant, *i.e.*, enhanced adsorption which, promoted its photocatalytic degradation.

Literature data suggest that organic acids may have a detrimental impact on TiNMs colloidal stability and promote aggregation. In the study reported by Pettibone *et al.*,[140] the adsorption of oxalic and adipic acid on 5 nm and 32 nm anatase TiNPs was investigated. Therein, the Langmuir adsorption parameters and surface-area-normalized coverages of both acids were deemed comparable. However, ATR-FTIR characterization revealed distinct molecular-level adsorption sites or configurations on smaller TiNMs, indicating that the aggregation dynamics and surface chemistry vary across the nanoscale. The extent of TiNMs aggregation is strongly pH-dependent, whereby the presence of organic acids destabilizes suspensions by altering the interparticle electrostatic interactions. On the other hand, aromatic organic acids, such as salicylic acid (SA), can potentially control the size of aggregates, as demonstrated in the paper by Almusallam *et al.*[30] Aggregates of TiNPs that have formed in the presence of 5 ppm SA had markedly reduced hydrodynamic radii in an acidic medium. Furthermore, the authors have determined that at 10 ppm SA, the aggregation process at pH 5 was effectively suppressed. Likewise, compounds such as tetraethylammonium hydroxide or

Tiron, which have demonstrated stabilization of TiNPs suspensions in water, are greatly impacted by the addition of ethanol. Lebrette *et al.*[141] have determined that ethanol, as cosolvent, can shift the slipping plane away from the particle surface and reduce the measured zeta potential in the case of TiNMs with Tiron or tetraethylammonium hydroxide. It was proposed that ethanol molecules fill the voids in water hydrogen-bond network, thereby moving the slipping plane away from the surface and decreasing repulsive interactions resulting in destabilization of the suspension if not carefully managed. The dependence of the TiNPs suspension stability of aqueous suspension in five different water chemistries regimes: (i) without additive, pH = 6.5; (ii) HCl and HNO_3, pH = 2.5, (iii) NH_3, pH = 9.5; (iv) 5 wt% ethylene glycol (EG); and (v) NH_3 + 5 wt% EG, pH = 9.5, was evaluated by UV-Vis spectrometry.[142] The latter one displayed the highest absorbance value, and the suspension remained stable for 4 days. The synergistic effect of the polyol molecule and the basic medium resulted in a higher efficiency of electrosteric repulsive forces compared with electrostatic or steric mechanisms.

Collectively, these findings reiterate how the interplay between pH, specific functional groups of organic and inorganic molecules as dispersants, and their concentrations determine the extent and nature of particle–particle interactions. Small molecules, such as catechol derivatives, amines, aromatic carboxylic acids as organic moieties, or inorganic ones, such as phosphates or silica coatings, can significantly enhance TiNMs colloidal stability by strong electrostatic and/or steric stabilization. Their effectiveness depends on matching dispersant chemistry with the surface properties of TiNMs. On the other hand, aliphatic organic acids[140] and inorganic phosphates[136] have been shown to destabilize TiNPs and nanosheet suspensions. Small organic molecules can provide either lipophilic (for example, oleic acid[138]) or hydrophilic (*i.e.* salicylic acid[30]) character of TiNMs, rendering good stability either in aqueous[37] or in organic medium.[143,144]

4.5. Natural organic matter

Understanding the interaction of nanomaterials with environmental components is crucial for understanding their fate in the environment, the potential risks they pose to nature and humans, as well as for utilizing their superior properties in various applications, including water protection and environmental remediation. In this sense, the interactions of nanomaterials with natural organic matter (NOM) are of special interest, as they can significantly influence the properties of nanomaterials. The importance of such investigations is evidenced by the development of the protocol preparation of nanoscale TiO_2 suspensions in an environmental matrix for ecotoxicological assessment.[145]

The stability of TiNMs in environmental waters is influenced by the concentration of the nanomaterial, as well as the physicochemical characteristics of the aqueous media. Primarily, various electrolytes (phosphate, sulfate, bicarbonate, chloride, *etc.*) and the pH value of the natural waters determine the extent of repulsion between the particles by electrostatic or electrosteric mechanisms, whereby the NOM macromolecules can either provide additional stabilization or cause aggregation, depending on the surface charge of the nano-TiO_2.[42,146,147] At a given pH value of the medium, the inverse value of Debye length ($1/\kappa$) is proportional to the valence charge of the electrolyte.[148] Therefore, an increase in the ionic strength of natural waters will compress the EDL and decrease zeta-potential, minimizing the repulsive forces between individual nanoparticles and ultimately increasing their aggregation. In addition, divalent cationic species present in natural waters reduce the zeta-potential more effectively than monovalent cations at pH value of the media above the pH_{pzc}, leading to the formation of larger agglomerates.[149,150] The studies have also demonstrated that the stability of TiNMs in natural waters is strongly influenced by the adsorption of various NOMs, organic sugars, carbohydrates, cellulosic materials, alginate, proteins, lipids, *etc.*, onto the particle surface. To model the fate of TiNMs in environmental waters, fulvic acid (FA), humic acid (HA) and sodium alginate are the most commonly used NOM model compounds. Due to the abundance of hydrophilic functional groups, these macromolecules can bind to the surface of TiNMs and thus strongly influence their stability. In particular, NOM molecules alter the surface properties of TiNMs by changing the surface charge, reactivity and aggregation behavior.[151] The studies investigating the stability of TiNMs in environmentally relevant conditions reviewed in this paper are summarized in Tables 5 and 6.

4.5.1. Humic substances. Humic substances (HS), a complex mixture of heterogeneous, high-molecular weight organic compounds of biotic origin, are omnipresent in soils, sediments and waters. HS are divided into humic acids (insoluble below pH = 2), fulvic acids (soluble in water regardless of pH), and humin (insoluble in water). Therefore, HA and FA are two common types of HS in the aqueous environments with different M_w and functional groups.[152]

Chen *et al.*[153] reported that they have obtained stable suspensions of anatase and rutile TiNPs in the presence of humic acid (HA). HA can stabilize TiNPs at a very low concentration mainly through increasing the electrostatic repulsion between particles. However, the stabilization mechanism also includes steric hindrance and hydrophobic interactions, although their effect is very weak. Due to the stability of the obtained suspensions, it is suggested that their photocatalytic efficiency may be high, thanks to an increase in surface area, which is of great importance for their applications. However, it was shown that the properties of the adsorbed NOM layer can influence the photocatalytic activity of TiNPs treated with phosphate. Although the degradation of model compound phenol was not affected, the degradation of its byproduct catechol could be enhanced or suppressed, depending on the adsorption conditions of NOM. This indicated that the influence of NOM on different reaction pathways should be considered.[154] Loosli *et al.*[155] confirmed that the presence of NOM in environmental concentrations induces significant deagglomeration of large submicron TiNPs agglomerates. Both electrostatic forces and steric interactions play important roles during this process.

Table 5 Summary of the reviewed studies investigating the stability of aqueous suspensions of TiO_2 nanomaterials (TiNMs) in the presence of humic substances

Dispersant[a] (concentration in solution)	TiNMs (w/v concentration in suspension)	Homogenization method	Ionic strength	pH	Ref.
HA (0.0001–0.002%)	Nanoparticles, anatase and rutile (0.01%; 0.02%)	Sonication, 15 min Shaking, 2 days	3 mM NaCl	4–8	153
Suwannee River NOM	Nanoparticles, mixture of anatase and rutile (0.00001%)	Rotation	10 mM phosphate	8	154
FA, HA (0.0001%, 0.001%)	Nanoparticles, rutile (0.001% 0.01%)	Shaker, 150 rpm, 48 h	0–50 mM $CaCl_2$	8	151
HA, TA (0.00001%, 0.00005% and 0.0001%)	Nanoparticles, P25 (0.00025%)	—	0.9 mM NaCl 0.3 mM $MgCl_2$ 0.3 mM $CaCl_2$	9	156
HA (0.00005%, 0.00025%, 0.0011%)	Nanorods, rutile (0.003%)	—	0.03 M NaCl 0.3 M NaCl	9.5–10.6 ($FeCl_3$) 7.0–10.8 (PFS)	157
HA (0.000057%; 0.00057%)E2 (0.0003%)	Nanorods, rutile (0.0005%)	Magnetic stir-plate, 30 s	100 mM NaCl 20 mM $CaCl_2$	7	42
Patented stabilizer SRHA (0–0.005%)	Nanoparticles, anatase (30%)	Dilution of stock solution	0–6 meq L^{-1} NaCl	3–4	158
SRHA (0.001%)	Nanoparticles, mixture of anatase and rutile (0.001%)	Sonication, 30 min	1, 10 and 100 mM NaCl and $CaCl_2$	5–9	159
HA (0.001–0.005%)	Nanoparticles (0–0.0025%)	Stirring overnight	100 mM NaH_2PO_4 100 mM NaCl	7.8	160
SRHA, SRFA, NOM (0.001–0.005%)	Nanoparticles, P25 (0.00005–0.00025%)	Stirring for 48 h	10–40 mM NaCl	7.9	161
NOM (conc. in natural waters)	Nanoparticles, P25 (0.0025%)	Sonication 30 min	5–100 mM NaCl 0.01–10 mM $CaCl_2$	9 different pH values	149
SRFA (10 ppm and 100 ppm)	Nanoparticles (20 ppm) (hydrothermal synthesis)	—	0–1200 mM NaCl 0–120 mM $NaNO_3$ 0–50 mM $Ca(NO_3)_2$ 0–16 mM $CaCl_2$	—	150
2,3-DHBA (0.05–3 mM) SRFA (0.9–10.9 mM)	Nanoparticles, anatase (hydrothermal synthesis)	Vortex 5 s	—	2.8	162

[a] 2,3-DHBA – 2,3-dihydroxybenzoic acid, E2 – 17β-estradiol, FA – fulvic acid, HA – humic acid, NOM – natural organic matter, SRHA – Suwannee River humic acid, SRFA – Suwannee River fulvic acid, TA – tannic acid.

Table 6 Summary of the reviewed studies investigating the stability of aqueous suspensions of TiO_2 nanomaterials (TiNMs) in the presence of non-humic substances and extracellular polymeric substances (EPS)

Dispersant[a] (concentration in solution)	TiNMs (w/v concentration in suspension)	Homogenization method	Ionic strength[b]	pH	Ref.
Alginate (0.00001%, 0.0001% and 0.001%)	Nanoparticles, P25 (0.0001%, 0.001%, 0.1%)	Sonication in ice bath (100 W, 20 min) + hand-shaking (60 s)	0.01 M Ca^{2+} 0.05 M Mg^{2+}	8.2	163
Alginate, HA, FA (0–0.08%)	Synthesized particles (0.02%)	—	0–300 mM NaCl 0–300 mM $CaCl_2$ 0–300 mM Na_2SO_4	2.5 12.0	164
Alginate (0.0003%) SRHA (0.0005%)	Nanoparticles, anatase (0.005%)	Dilution from stock solution	0.001 M NaCl	6.2	155
Alginate, SRHA (0.01%)	Nanoparticles, anatase (0.005%)	Dilution from stock solution	0.001 M NaCl	2–11	165
Alginate (0.0001–0.001%)	Nanoparticles, anatase (0.005%)	Dilution from stock solution	0–0.1 M NaCl 10^{-1}–10^{-5} M $CaCl_2$	4.5 9.2	166
BAD (0.00025%)	Nanoparticles, anatase (0.0005%)	Sonication	50–300 mM NaCl	3 9	167
EPS from *B. subtilis* (0.002%)	Nanoparticles, anatase (0.01%)	Magnetic stirrer, 20 min	1–500 mM NaCl 0.05–40 mM $CaCl_2$	8.0	168
EPS from *B. subtilis* (0.02%)	Nanoparticles, anatase (0.5%)	Magnetic stirrer, 20 min	0–1500 mM NaCl	3–10	169
EPS from *E. coli* (0–0.025%) EPS from *Chlorella pyrenoidosa* (0–0.025%)	Nanoparticles, anatase and rutile (0.1%)	Sonication, 20 min at 25 °C	150 mM NaCl	7.5	170
EPS from *E. coli*	Synthesized, rhomboedric (anatase), cubic (anatase), elongated (rutile) (0.1%)	Sonication, 30 min	171.5 mM PBS	7.2	171
EPS from *C. vulgaris* (0–0.005%)	Nanoparticles P25 (0.2%)	Sonication, 30 min	0–70 mM NaCl 0–50 mM $CaCl_2$	—	172
EPS from *C. reinhardtii* (0–0.0005%) EPS from *D. tertiolecta* (0–0.0005%)	UV100 (anatase), M212 (rutile) and M262 (rutile) (0.05%)	Sonication, 1 h	0–800 mM NaCl	3–11	173

[a] BAD – benzyl-grafted alginate derivative, EPS – extracellular polymeric substances, HA – humic acid, FA – fulvic acid, NOM – natural organic matter, SRHA – Suwannee River humic acid. [b] PBS – phosphate buffer saline.

Recently, Luo *et al.*[151] demonstrated that HA and FA can adsorb to the surface of rutile TiNPs, altering their hydrophilic-hydrophobic balance and thus playing an important role in colloidal stability. Due to the difference in hydrophobic group content and molecular weight, the adsorption percentage of HA was twice that of FA. It was shown that at IS < CCC, both FA and HA stabilize the TiNPs, whereas at IS > CCC, a destabilization occurs. This suggests that NOM entanglement and NOM bridging are possible mechanisms of interaction with TiNPs. In a study conducted by Romanello and coworkers[156] HA and tannic acid (TA) were found to have a stabilizing effect on TiNPs through adsorption on their surface when the IS was adjusted to 0.9 mM and at different aqueous pH. The adsorption of negatively charged HA stabilized TiNPs over a wider pH range (2–9) compared to the neutral TA form (pH values below or above $pH_{PZC} = 4$), in accordance with the DLVO theory. However, the stabilization effect of both HS could be affected by divalent calcium cations in the concentration range of 0.3–1.5 mM, which is due to the formation of Ca^{2+}-NOM bridges. The study by Lee *et al.*[42] investigated the aggregation of rutile TiO_2 (5 mg L^{-1}) in the presence of HA and/or 17β-estradiol (E2) under high ionic conditions. The results showed that HA alters the surface charge more than E2 and, therefore, plays a more important role in the aggregation behaviour of TiNPs.

Hsiung *et al.*[158] investigated the aggregation and sedimentation of commercial anatase TiNPs under different pH, ionic strength (NaCl), and Suwannee River humic acid (SRHA) concentrations. The stability of TiNPs was independent of their concentration. However, aggregation occurred at a pH near pH_{PZC}. As expected, the aggregation was enhanced by the presence of NaCl due to EDL compression. The stability of TiNPs at low and high SRHA, accompanied by charge reversal, suggests that charge neutralization is responsible for the destabilization of the suspensions. Another stability study on the impact of the SRHA on stability of TiNPs was carried out by Thio *et al.*[159] The presence of SRHA significantly increased the stability of TiNPs over a broad range of IS (1 mM and 10 mM) and pH (5–9). Aggregation of TiNPs occurred only in highly saline environments (IS > 200 mM NaCl and > 5 mM $CaCl_2$ electrolyte).

Erhayem and Sohn[160] investigated the stability of TiO_2 particles upon adsorption of HA from different sources and naturally occurring organic matter (NOOM, which includes HA, FA and NOM).[161] Low HA concentrations destabilize the TiNPs particles even in the absence of background electrolyte, but they prove to be effective stabilizers in higher concentration regimes (≥25 mg L^{-1}) up to 100 mM NaCl.[160] The increase in nano-TiO_2 aggregation was observed at a NOOM concentration of 10 mg L^{-1} at a pH of 7.9 and ionic strength of 4.6 mM, while aggregation decreased when the NOOM concentration was increased up to 25 mg L^{-1}. Furthermore, the authors have shown that the adsorption of NOOM follows Freundlich isotherms. The NOOM species with greater hydrophobicity and higher M_w values, such as HA, have a greater affinity to adsorb onto the TiNPs, leading to an increase of K_{ads} in either acidic or basic media.[161] Ottofuelling and co-workers[149] reported a comprehensive study on the colloidal stability study of commercial TiO_2 NPs (P25) in various aqueous matrices, *i.e.*, synthetic waters (using standard electrolyte solutions), natural waters (groundwater, lake water, tap water, wastewater, *etc.*), and standard synthetic (EPA) waters, showing that the presence of NOM does not have an unidirectional stabilizing effect. In natural waters with low mineral content, stabilizing effect was greater than in waters with higher NOM content. In the EPA, the TiNPs stability decreased with increasing pH and IS value.

Majority of studies of the fate of TiNMs in environmental waters focus on the influence of ionic strength and diverse stabilizing agents, neglecting the effects of NMs morphologies. To address this limitation, Raza and co-authors[150] investigated the impact of different dispersant concentrations, pH values, and ionic strengths on the aggregation kinetics of ellipsoidal and spherical TiNPs. Of the five dispersants used, PEG, PVP, SDS, citrate and Suwanee river fulvic acid (SRFA), the latter two were the most effective in terms of suspension stability, shifting the pH_{PZC} value of the spherical anatase particles from pH = 5.6 (bare particles) to the value of 1.6 in the presence of citrate and 2.3 in the presence of SRFA, respectively. It was also found that the two morphologies studied were less stable in the presence of calcium salts (chloride and nitrate) than in the presence of sodium salts (chloride and nitrate), due to the formation of stable complexes between the Ca^{2+} ions and the carboxyl groups of the dispersants, resulting in lowering the CCC value. In general, both types of NPs were relatively more stable in the presence of SRFA than in the presence of citrate, mainly due to the hydrophobicity and compact conformation of SRFA molecules on the TiNPs surface, resulting in stronger electrosteric repulsion. Under the same conditions, SRFA-stabilized ellipsoids were more stable than the SRFA-stabilized spheres. These morphology-related properties are the result of different SRFA conformations on the surface of TiNPs. A more compact layer forms on the spheres, while more extended chains are present on the surface of the ellipsoids.

Despite the need to assess the long-term stability of TiNMs in environmental conditions, in order to assess their environmental impact, such studies are rare. Danielsson *et al.*[162] studied the stability of TiNPs in the presence of 2,3-dihydroxybenzoic acid (2,3-DHBA), model phenolic carboxylic compound, and SRFA during 9 months at pH 2.8 of relevance for acid mine drainage sites. Depending on the 2,3-DHBA concentration, during first month zeta potential of TiNPs decreased with time, resulting in surface charge neutralization at 2,3-DHBA concentration 1.5 mM and charge reversal at higher concentrations. After 1 month, zeta potential decreased only slightly. Accompanying the changes in zeta potential, at 2,3-DHBA concentrations above 0.1 mM, the hydrodynamic diameter of the aggregates increased in the first month to several microns. After this initial increase, the diameter of aggregates decreased to several hundred nanometres after 9 months. It was suggested that the initial adsorption of 2,3-DHBA can be fast. With time, the slower rearrangement of initially formed surface complexes occurs, resulting in changes in zeta potential and, consequently, aggregation behaviour. Different behaviour was observed in the presence of SRFA. The zeta potential of TiNPs didn't change significantly, indicating

negligible interaction of TiNPs and SRFA, possibly due to the low SRFA concentration investigated (up to 12 μM). Consequently, only a slight increase in TiNPs' hydrodynamic diameter was observed. However, increasing SRFA's concentrations to 20–80 μM, resulted in an increased amount of SRFA adsorbed to the surface of TiNPs and destabilization of the system for 7 days.

In the search for an effective method of removal of NMs from waters, the feasibility of iron-based coagulants, poly-ferric sulfonate (PFS) and ferric chloride ($FeCl_3$), to remove rutile TiNPs from the aqueous phase in the presence of HA was tested.[157] The results showed that at low alkalinity of media, and in the presence of $FeCl_3$, HA exceptionally stabilized TiNPs in the entire tested concentration range (0.5–11 mg mL^{-1}), with the zeta potential remaining very high (+40 mV). On the other hand, the presence of PFS was effective in destabilizing TiNPs at lower HA concentrations (up to 2.5 mg mL^{-1}).

4.5.2. Non-humic substances. Non-humic substances include low-molecular weight compounds such as carbohydrates, proteins, lipids, and sugars. In this chapter, the influence of alginates and their derivatives on the colloidal stability and environmental fate of TiNMs is highlighted. Alginates, linear chains of anionic polysaccharides consisting of (1→4)-linked α-L-guluronic acid and β-D-mannuronic acid repeating units in random arrangement, are natural compounds isolated from brown algae (Phaeophyceae).[174] Alginates can be further modified in aqueous and organic media to tailor their properties for final application.[175]

Callegaro *et al.*[163] reported on the stability of pristine P25 TiNPs in artificial seawater under different probe-sonication regimes and varying alginate concentrations. Prolonged sonication resulted in an increase in the hydrodynamic radius of aggregates, indicating that the alginate coating was partially removed from the particle surface. The most effective stabilization occurred at an alginate concentration of 0.45 g L^{-1}, as the highly saline medium of the artificial seawater promoted flocculation of the polysaccharides in the higher concentration regimes investigated.

Three types of macromolecules (alginates, HA and FA) and three types of electrolytes (NaCl, Na_2SO_4 and $CaCl_2$) were evaluated in terms of the stability of TiNPs prepared by a wet-chemical process at pH = 2.5 (positively charged particles) and pH = 12 (negatively charged particles).[164] The stability of TiNPs was strongly dependent on: (i) the degree of coverage as sufficiently encapsulated particles were protected from aggregation, even at higher IS; (ii) the mixing conditions and initial NOM concentrations, which were crucial for the sorption of natural macromolecules; and (iii) M_w of NOM as larger molecules provided an additional steric hindrance in the presence of sodium chloride and sulphate, but were strongly destabilized in the presence of Ca^{2+} due to the bridging of macromolecules.

Several studies on the disagglomeration of manufactured TiNPs in the presence of NOMs under realistic environmental conditions were carried out by the Stoll group.[155,165,166] It was shown that at a pH corresponding to the point of zero charge (pH = 6.2) and an initial TiNPs concentration of 50 mg L^{-1}, negatively charged alginates and SRHA natural polyelectrolytes can bind to the surface of titania agglomerates and successfully promote deagglomeration to smaller particles, *i.e.* redispersion of titania particles.[155] The authors have shown that the disagglomeration process was governed by the adsorption of NOM macromolecules as well as their ability to reach the internal structure of the agglomerates. Compared to the semi-rigid globular SRHA conformation, alginate, as a semi-rigid, linear polysaccharide with a homogeneous charge distribution, can easily change its conformation and, therefore, had a greater deagglomeration ability. Although a lower concentration of alginate was required to achieve maximum deagglomeration than SRHA, the larger electrostatic repulsive forces can restabilize TiO_2 particles more effectively, resulting in smaller SRHA-TiNPs clusters. The influence of NOM on the colloidal titania stability was also investigated in a broader pH range.[165] At a pH of water media below the pH_{PZC}, rapid adsorption of negatively charged alginates and SRHA to the positively charged titania surface occurred. If the aqueous pH was above the pH_{PZC}, all components were negatively charged. Therefore, the adsorption of NOM was minimal. The stability of TiNPs was also studied in the presence of NaCl (up to 0.1 M) and $CaCl_2$ (10^{-1}–10^{-5} M) at two pH of interest: (i) pH = 4.5 (pH < pH_{PZC}); and (ii) pH = 9.2 (pH > pH_{PZC}).[166] The higher affinity of Na^+ to disrupt colloidal stability was observed in an alkaline medium. Lower CCC and zeta-potential values in the diffusion-limited aggregation domain confirmed the formation of larger aggregates. Due to the specific adsorption of Ca^{2+} onto the negatively charged

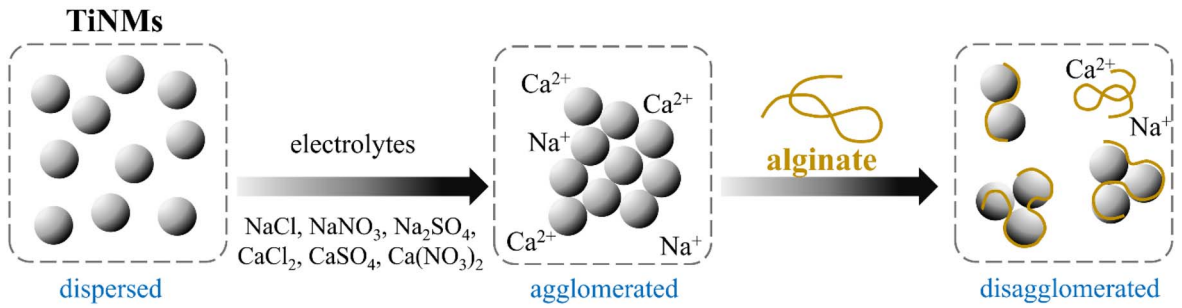

Fig. 8 Schematic presentation of disagglomeration and stabilization of TiO_2 nanomaterials (TiNMs) by alginates. Adapted from ref. 166 with permission from Elsevier Ltd.

TiNPs, the disruption of colloidal stability was even more pronounced, rendering the CCC value three orders of magnitude lower than that obtained in the presence of NaCl. The impact of alginate (γ = 1–10 mg L^{-1}; pH = 8.2) was further investigated in the presence of Ca^{2+} (45 mg L^{-1}) and Mg^{2+} (5 mg L^{-1}). It was shown that increasing the polysaccharide concentration up to $\gamma \geq 8$ mg L^{-1} significantly promoted the deagglomeration of larger clusters, reducing their size from micrometre to smaller nanometre sized fragments. A schematic representation of larger titania cluster disagglomeration and stabilization of smaller TiNMs units by alginate dispersant is given in Fig. 8.

An improvement in colloidal stability was achieved by the introduction of benzyl-grafted alginate derivative (BAD) as the dispersing agent for anatase type TiNPs.[167] BAD molecules consist of hydrophobic main chains and hydrophilic side groups. In an aqueous medium, they form micelle-like self-aggregates with exposed hydroxyl groups, which are available for adsorption on the TiNPs surface. The BAD/TiNPs complex exhibited a zeta-potential value of −36.4 mV, indicating good colloidal stability. This was also confirmed by DLS measurements, which indicated a decrease in the average hydrodynamic diameter by several orders of magnitude over a wide pH range (pH = 3–9). Moreover, the BAD/TiNPs complex was more resistant to the IS changes than the pristine TiNPs, although the monovalent sodium ion serves as a counterion to the negatively charged oxo/carboxyl species inducing the aggregation of the particles.

The studies reviewed in last two sections reveal that the stability of TiNMs in environmental waters is influenced by the concentration of the nanomaterial and particle morphology,[150] as well as the physicochemical characteristics of the aqueous media.[149] Primarily, various electrolytes (phosphate, sulfate, bicarbonate, chloride, *etc.*) and the pH value of the natural waters determine the extent of repulsion between the particles by electrostatic or electrosteric mechanisms, whereby the NOM macromolecules can either provide additional stabilization or cause aggregation, depending on the surface charge of the nano-TiO_2.[42,146,147] At a given pH value of the medium, the inverse value of Debye length ($1/\kappa$) is proportional to the valence charge of the electrolyte.[148] Therefore, an increase in the ionic strength of natural waters will compress the EDL and decrease zeta-potential, minimizing the repulsive forces between individual nanoparticles and ultimately increasing their aggregation. In addition, divalent cationic species presenting natural waters reduce the absolute value of zeta-potential more effectively than monovalent cations at pH value of the media above the pH_{PZC}, leading to the formation of larger agglomerates.[149,150] The studies have also demonstrated that the stability of TiNMs in natural waters is strongly influenced by the adsorption of various NOMs, organic sugars, carbohydrates, cellulosic materials, alginates, proteins, lipids, *etc.*, onto the particle surface. To model the fate of TiNMs in environmental waters, fulvic acid (FA),[151,164] humic acid (HA)[151,153,156] and sodium alginate[163,166] are the most commonly used NOM model compounds. There are also studies including standard Suwanee river humic acid (SRHA)[158] or Suwanee river fulvic acid (SRFA)[150] macromolecules as a model NOM compounds. Due to the abundance of hydrophilic functional groups, mainly of carboxylic and hydroxyl type, these macromolecules can bind to the surface of TiNMs and thus strongly influence their stability.[161,165,167] In addition, NOM species also contain (abundant) hydrophobic groups (mostly alkanes and aromatic hydrocarbons), which contribute to the π–π stacking.[151,157] Unlike the binding of small molecules, adsorption of NOM molecules onto the nano-TiO_2 surface usually occurs through the joint effect of electrostatic, hydrophilic and hydrophobic interactions.[162] The formation of NOM corona layer may contribute to the high colloidal stability even under high ionic strength, as it was shown for humic acid-coated TiO_2,[159] SRHA-encapsulated particles[161] or BAD/nano–TiO_2 complex.[167] It is suggested that an increment in IS leads to the NOM conformation change to more compact form. Consequently, the greater amount of macromolecule stabilizers can adsorb to the TiNMs surface, generating enhanced steric hindrance. Although long-term stability (up to 9 months) was achieved in a batch experiment with 2,3-DHBA as TiO_2 stabilizer in acidic media (pH = 2.8),[162] understanding the colloidal stability and ultimate fate under the environmentally realistic conditions (neutral or slightly basic pH, adjusted IS, hardness and NOM content) still presents an important challenge.[149,150] Even though abundance of NOM molecules in natural environments would act as stabilizers and thus increase the colloidal stability, the presence of other (complex) ions, chemical species and/or biological debris may completely change particle mobility and stability. In summary, NOM molecules alter the surface properties of TiNMs by changing the surface charge, reactivity and aggregation behaviour.[151]

4.5.2.1. Extracellular polymeric substances. Extracellular polymeric substances (EPS) are a specific class of NOM species produced solely by microorganisms.[166] This heterogeneous mixture of biological macromolecules, consisting mainly of polysaccharides, proteins, nucleic acids and lipids, covers the microbial cell surface, and forms the matrix of the biofilm in the environment.[170] In natural ecosystems, EPS can interact with various engineered nanomaterials, influencing their environmental behaviour and toxicity.[176] In the previous section influence of model EPS molecule alginate has been reviewed. In this section scientific papers investigating the nano-TiO_2 colloidal stability in the presence of EPS extracted from different bacteria and algae are reviewed (Table 6). A detailed discussion of the interaction mechanisms between TiNMs and the corresponding EPS macromolecules is provided below.

The adsorption of EPS extracted from *Bacillus subtilis* onto the TiO_2 surfaces, along with its effect on the colloidal stability and aggregation behaviour of TiNPs, was investigated by Lin and co-workers.[168,169] The aggregation behaviour of TiNPs examined in electrolyte solutions of various IS (1–500 mM NaCl and 0.05–40 mM $CaCl_2$, respectively), and at a constant pH value of 8, was in agreement with the classical DLVO theory.[168] In other words, the results showed that the divalent cations disrupted colloidal stability more efficiently than monovalent electrolytes, rendering lower CCC values (1.3 mM $CaCl_2$ *vs.* 11 mM NaCl). Nonetheless, the addition of EPS in the lower concentration regimes (*i.e.* <10 mM for NaCl and <1 mM for

$CaCl_2$) resulted in enhanced steric repulsion, which effectively stabilized the TiNMs. In the following study, the authors further examined the role of pH in the aggregation of TiNMs, by changing the pH of the medium from acidic to alkaline.[169] At pH = 4 (<pH_{PZC}), at an EPS concentration below 0.1 mg L^{-1}, a stable colloidal dispersion of positively charged particle aggregates with an average hydrodynamic diameter of 300 nm was observed. Increasing the EPS concentration (up to 0.6 mg L^{-1}) led to rapid aggregation of titania clusters, *i.e.* colloidal instability, accompanied by a steep drop in zeta-potential value, charge inversion, and a sudden increase in hydrodynamic radius (d_h = 1500 nm). A further increase in EPS concentration (>0.6 mg L^{-1}) led to re-colloidal stabilization, TiNPs had negative zeta-potential values and a corresponding average cluster diameter of d_h = 213 ± 15 nm. At pH_{PZC} (pH = 6.0), the aggregation rate reached a maximum value, but the adsorption of EPS led to partial fragmentation by electrostatic repulsion. When the pH was greater than pH_{PZC} (pH = 8), the aggregation rate was only minimally affected by the increase in EPS concentration.

Several studies on the adsorption of EPS from different microbes onto the anatase (nTiO_2-A) and rutile (nTiO_2-R) crystal forms, as well as insights into the interactions of nano-TiO_2 and algal cells, were conducted by the Lin group.[170,177,178] EPS extracted from *Escherichia coli* (E-EPS), which are mainly composed of proteins with relatively high M_w and pronounced aromaticity, were responsible for the increase in colloidal stability, providing long-range steric hindrance.[170] On the other hand, EPS extracted from *Chlorella pyrenoidosa* (C-EPS), which hydrophilic polysaccharide components have lower M_w, had limited adsorption on the TiO_2 surface and consequently led to colloidal instability. The adsorption of E-EPS and C-EPS was controlled by the active surface area of the crystalline form studied, with the rutile TiO_2 form exhibiting the highest adsorption per unit area. A schematic representation of EPS extraction from algae and bacteria and the stabilization of nTiO_2 with proteins and polysaccharide dispersants is shown in Fig. 9. This research was the basis for exploring the toxic effects of different crystallographic TiO_2-forms on the algal regulation mechanisms, as well as on the microbial community.[177,178]

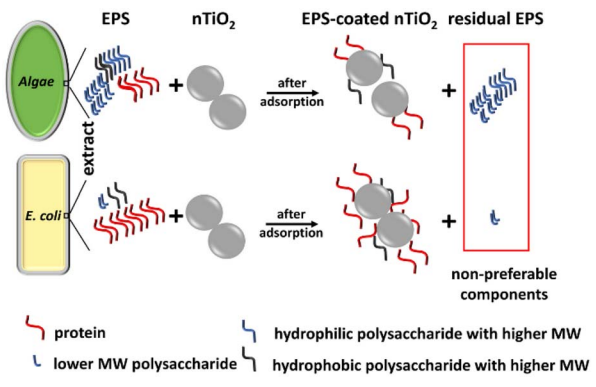

Fig. 9 Adsorption of EPS from algal and bacterial sources on nTiO_2 particles. Reproduced from ref. 170 with permission from Elsevier Ltd.

The formation of EPS corona (composed mostly of proteins extracted from *E. coli*) on TiO_2 of different crystalline phases and exposed facets, namely A_101, A_001 and R_110, was studied by Du *et al.*[171] Each crystalline phase exhibited different physicochemical properties that determine the extent of their interactions with macromolecules. Due to the octahedral morphology, the A_101 particles formed the largest aggregates (1310 nm) and exhibited the most negative surface charges, which may influence the electrostatic interactions with EPS. On the other hand, A_001 particles had the highest surface hydroxyl density, prone to H-bonding formation, while R_110 particles had the largest hydrophobicity. Therefore, the selective adsorption of EPS proteins was determined by hydrogen bonding and hydrophobic interactions with anatase particles, while hydrophobicity was the major interaction in the formation of the EPS corona on the rutile particles. The EPS corona of the three crystal forms differed significantly in thickness, as well as in protein content. 39 proteins were selectively adsorbed only in A_001 NPs, 100 were found specifically in A_001 grains and 117 were characteristic for R_110 particles, respectively. The results pointed out that the crystalline phase and exposed facets induced pronounced variations in the abundance of proteins in EPS coronas, which affects the environmental fate of TiNMs.

The colloidal stability and aggregation kinetics of P25 nano-TiO_2 were investigated in the presence of EPS extracted from the alga *Chlorella vulgaris* (concentrations of 1 mg L^{-1}, 3 mg L^{-1} and 5 mg L^{-1}), monovalent NaCl (1–60 mg L^{-1}) and divalent $CaCl_2$ (0.1–10 mg L^{-1}) electrolytes.[172] The study revealed that the coexistence of EPS and divalent Ca^{2+} promoted aggregation and sedimentation of TiNPs due to the intermolecular bridging between the cation and the carboxylic groups of polysaccharides. The presence of EPS in the background electrolyte (5 mM NaCl) led to an increase in stability and shifted the CCC value from 11.07 mM (only NaCl) to 14.99 mM (3 mg per L EPS) and 23.16 mM (5 mg per L EPS), respectively. This reduction in aggregation observed in NaCl containing matrices is attributed to the strong electrostatic repulsions between EPS-coated TiNMs.

The colloidal stability of TiNMs was also studied with regard to two soluble EPS (sEPS) species, one produced from the marine alga *Dunaliella tertiolecta*, and the other from freshwater phytoplankton *Chlamydomonas reinhardtii*.[173] This research, carried out with the three commercial TiNMs, *i.e.* UV100 (uncoated spherical particles), M212 (hydrophilic cubic particles coated with alumina and glycerol) and M262 (hydrophobic elongated particles coated with alumina and dimethicone polymer), showed that the adsorption of sEPS was dependent on particle morphology, surface charge, and hydrophobicity. The CCC of all TiNPs increased in the presence of sEPS from both freshwater and marine sources. The highest colloidal stability was achieved with M262 particles coated with sEPS isolated from *D. tertiolecta*. It was suggested that the attachment of sEPS to the hydrophobic TiO_2 coating significantly alters its surface chemistry and improves the stability in water.

Different chemical (pH and IS) and/or environmental conditions (presence of other inorganic species or NOM

substances) can change the conformation and protonation state of EPS functional groups, initially altering their adsorption rate onto the TiO_2 surface and, consequently, the colloidal stability. In the original scientific papers summarized in this review, EPS were mostly extracted from bacteria[168,169,171] and algae.[170,177,178] In general, EPS can adsorb onto the TiO_2 surface through various interaction mechanisms: electrostatic attraction or repulsion, chemical or hydrogen bonding, hydrophobic interactions, and cation bridging.[179] Since TiNMs are negatively charged in natural waters, electrostatic attraction with oppositely charged particles, *i.e.*, positively charged EPS functional groups, was found to be the predominant interaction mechanism.[176] Furthermore, chemical bonding was also found to be one of the most important interaction mechanisms for EPS sorption on the nano-TiO_2 surface. Due to the abundance of functional groups and the diversity of EPS, in most cases combined interaction mechanisms are involved in the formation of the EPS corona, electrostatic interactions and chemical bonding between the COO^- groups of the TiNMs and the sEPS molecules,[173] hydrophobic interactions between aromatic protein moieties coupled with hydrogen bonding between surface hydroxyl groups and amino groups of the EPS species,[170] or joint electrostatic interactions and H-bonding, due to the high content of EPS amino-acids with charged functional groups.[171] Classical thermodynamic models are considered to be suitable for describing the adsorption of EPS on the nano-TiO_2 surface, usually fitted using the Langmuir equation.[169,170]

Once released into aquatic ecosystems, TiNMs inevitably interact with other biogenic and geogenic substances, including EPS. The formation of an EPS corona significantly alters the TiNMs surface chemistry, leading to aggregation (colloidal destabilization) or disaggregation (colloidal stabilization) processes, consequently affecting the environmental fate and toxicity.[180]

5. Application of stabilized TiO_2 nanomaterials suspensions

TiNMs are being tested or are already in use for a wide range of applications, including UV light absorption, coatings, painting pigments, photosynthesis, flame retardancy, photocatalysis, the ceramic industry, antimicrobial and antioxidant agents, and medical implants.[4,5,67,181–183] In many of them, TiNMs are used in the form of stable suspensions, which are subsequently applied to flexible or rigid substrates using various techniques in the form of a thin film. When formulating the stable suspension, one should keep in mind that the presence of dispersant could alter the physico-chemical properties of TiNMs on which the application is based.

Leong *et al.*[184] investigated the ability of TiNPs thin films immobilized onto a glass substrate for the photocatalytic self-cleaning of indoor air pollutants. It was demonstrated that TiNPs in concentrations exceeding 15 g L^{-1} can form a uniform, thin layer on glass surfaces and enhance the photodegradation of formaldehyde under UV light. Another study investigated TiNPs self-cleaning coatings on the clothing fibers.[112] It was shown that the photocatalytic activity of the prepared coating depends on the thickness and uniformity of the coating layers, which are affected by the stability of the bulk suspensions. In this study, dimeric surfactants were used, and their presence improved TINPs suspensions' stability and coatings' thickness. Othman *et al.*[40] tested different formulations of TiNPs aqueous suspensions stabilized with PAA for glass coating. It was found that the optimal PAA concentration is 3 wt% improves Ti surface concentration and uniformity of TiNPs layers on a glass substrate. Li *et al.*[185] also proposed a formulation of SiO_2/TiO_2 nanocoatings for photocatalytic self-cleaning, enhanced transmittance, and antireflection of solar cell devices, windows, *etc.*, which were applied as ethanolic suspension. The optimal formulation developed within this study provided the balance between the photocatalytic and optical properties of the obtained coatings.

Concentrated TiNPs suspensions for waterborne coating preparation were also prepared, using PMS (P(MMA-MPS)) copolymer nanospheres (from methyl methacrylate (MMA) and γ-methacryloxypropyltrimethoxysilane (MPS)) as stabilizing agent. PMS nanospheres showed good stabilizing performance, and enabled the preparation of highly concentrated TiNPs suspensions without the high increase in suspension viscosity and good storage stability up to 28 days.[186]

Another potential application of TiNPs is the preparation of antibacterial surface coatings. Singh *et al.*[187] tested the antibacterial activity of TiNPs coatings on black silicon, and obtained a good antibacterial effect in terms of significant reduction of CFU mL^{-1}, which can be further improved by modifying the surface topology and coating technique.

The influence of the shape of TiNMs on UV light absorbance was also investigated. The study examined the UV-protective effects of TiO_2 nanotubes, nanoplates, and nanowires. It was concluded that nanoplates and nanowires were significantly more effective in protecting against UVB irradiation compared to nanotubes.[188]

TiNMs stabilized with NaPAA were also tested as additives to enhance the lubrication and tribological properties of pure water. The obtained results indicated that TiNPs suspensions with NaPAA show good tribological performance, as well as the performance, is dependent on both TiNPs and NaPAA concentrations.[189]

It was also suggested that TiNPs could be used for the formulation of nanoelectrofuels, and serve for energy storage or catalysis.[92] TiNMs' photocatalytic activity can also be employed for the removal of micropollutants from water.[190] The composite of rutile and anatase crystalline forms, were synthesized for photocatalytic degradation of organic pollutants.[191] The prepared composite exhibited exceptional photocatalytic performance, achieving a rapid degradation rate of 99.0% for a methyl orange solution during 30 min under UV light. Another example of the potential use of TiNPs suspensions is for water depollution presented by Ko *et al.*[192] Authors tested the efficacy of TiNPs photocatalytic depollution on three organic model pollutants under UV irradiation. It was shown that the pore size and crystalline structure of TiNPs affect the efficiency of photocatalytic degradation of organic pollutants.

Leu *et al.*[193] designed a new polymeric dispersant, branched poly-(oxyethylene)-segmented esters of trimellitic anhydride adduct (poly-ethylene glycol-trimethylolpropane-trimellitic anhydride) in order to prepare homogenous TiNPs suspensions. They further prepared films of photoanodes for dye-sensitized solar cells, which were more efficient than conventional TiO_2 photoanodes.

One of the most common commercial uses of TiNPs is in the form of a spray or an aerosol. However, the physicochemical properties of nanoparticles in suspension before spraying and in aerosol after spraying could differ. The study conducted by Park *et al.*[194] showed that the particle diameter was larger after spraying, compared to suspended particles, which was interpreted as a result of particle aggregation during passing through the nozzle. Another common use of TiNMs is as pigments in ink suspensions, which requires good colloidal stability. Cran *et al.*[124] used different dispersants in order to improve the stability of commercially available pigment nanoparticles – aluminate- and zirconia-coated rutile TiNPs. The study demonstrated that negatively charged dispersants provide both electrostatic and steric stabilization for the aforementioned commercial pigment particles. Nowadays, TiO_2 is commercially used in a large number of food and personal care products. Among the others, personal care products with the highest TiO_2 content are toothpastes and sunscreens (with 1–10% TiO_2), while the foods with the highest TiO_2 content include chewing gums and candies. The food-grade TiO_2 is labelled as food additive E171.[17]

6. Conclusions

The constantly increasing use of TiO_2 nanomaterials raises questions about the preparation of more efficient products, on one hand, and the safety of their application on the other. Understanding the mechanisms that govern the stability of TiNMs in various media, most notably aqueous, and in the presence of different dispersants, is crucial for answering both questions. This motivates investigations into the stability of TiNMs suspensions in rather different conditions, chosen depending on the final application. Interactions between TiNMs and dispersants can be complex, even in simple systems. The majority of the experimental results can be theoretically explained by DLVO theory despite its drawbacks. However, the choice of the right dispersant and final formulation is still mostly subject of a trial-and-error procedure. Combining DLVO with other models of surface interactions could provide additional insights and facilitate the easier design and synthesis of dispersants tailored for specific applications. It should be considered, that the influence of dispersants on intended applications should be carefully considered, as their presence can alter the properties of TiNMs.

Among the advantages of TiNMs is the possibility of preparing them not only in different compositions but also in various morphologies, which can influence TiNMs' properties and, consequently, the properties of the final product. However, investigations into the influence of dispersants on the stability of suspensions of TiNMs, other than TiNPs, are scarce.

The studies reviewed in this paper contribute to the development of environmentally safe and efficient products in an environmentally friendly manner.

Data availability

No primary research results, software or code have been included and no new data were generated or analysed as part of this review.

Author contributions

Ljiljana Spasojević: visualization, writing the original draft, writing review & editing. Irena Ivanišević: conceptualization, visualization, writing the original draft, writing review & editing. Maja Dutour Sikirić: conceptualization, funding acquisition, project administration, writing the original draft, writing review & editing.

Conflicts of interest

There are no conflicts to declare.

Acknowledgements

This work was financially supported by the European Union's Horizon-RIA project, Surface Transfer of Pathogens (STOP), Grant agreement ID: 101057961. Lj. S. received financial support of the Croatian Science Foundation, Grant agreement: MOBDOL-2023-08-2261.

References

1 F. Piccinno, F. Gottschalk, S. Seeger and B. Nowack, *J. Nanopart. Res.*, 2012, **14**, 1109.
2 X. Bian, J. Wang, Y. Bai, Y. Li, W. Wu and Y. Yang, *Catalysts*, 2024, **14**, 558.
3 C. Revilla, A. Challco, K. Tejada, R. Terán, K. Garcia and G. Colina, *Environ. Technol. Innovation*, 2025, **37**, 104030.
4 I. Ali, M. Suhail, Z. A. Alothman and A. Alwarthan, *RSC Adv.*, 2018, **8**, 30125–30147.
5 X. Chen and S. S. Mao, *Chem. Rev.*, 2007, **107**, 2891–2959.
6 M. B. K. Suhan, M. R. Al-Mamun, N. Farzana, S. M. Aishee, M. S. Islam, H. M. Marwani, M. M. Hasan, A. M. Asiri, M. M. Rahman, A. Islam and M. R. Awual, *Nano-Struct. Nano-Objects*, 2023, **36**, 101050.
7 D. Kışla, G. G. Gökmen, G. Akdemir Evrendilek, T. Akan, T. Vlčko, P. Kulawik, A. Režek Jambrak and F. Ozogul, *Trends Food Sci. Technol.*, 2023, **135**, 144–172.
8 M. F. Kunrath, R. Hubler, R. S. A. Shinkai and E. R. Teixeira, *ChemistrySelect*, 2018, **3**, 11180–11189.
9 F. Zuo, Y. Zhu, T. Wu, C. Li, Y. Liu, X. Wu, J. Ma, K. Zhang, H. Ouyang, X. Qiu and J. He, *Pharmaceutics*, 2024, **16**, 1214.
10 T. da Silva Dassoler, E. de Sousa Cordeiro, D. Hotza and A. De Noni Junior, *Open Ceram.*, 2023, **13**, 100331.

11 J. A. Benavides-Guerrero, L. F. Gerlein, C. Trudeau, D. Banerjee, X. Guo and S. G. Cloutier, *Sci. Rep.*, 2022, **12**, 15441.
12 I. C. R. Gomes, K. J. Ciuffi, L. Marçal, L. A. Rocha and E. J. Nassar, *J. Coat. Technol. Res.*, 2024, **21**, 1483–1498.
13 J. Jenima, M. Priya Dharshini, M. L. Ajin, J. Jebeen Moses, K. P. Retnam, K. P. Arunachalam, S. Avudaiappan and R. F. Arrue Munoz, *Heliyon*, 2024, **10**, e39238.
14 C. Cazan, A. Enesca and L. Andronic, *Polymers*, 2021, **13**, 2017.
15 A. Mansoor, Z. Khurshid, M. T. Khan, E. Mansoor, F. A. Butt, A. Jamal and P. J. Palma, *Nanomaterials*, 2022, **12**, 3670.
16 D. Ziental, B. Czarczynska-Goslinska, D. T. Mlynarczyk, A. Glowacka-Sobotta, B. Stanisz, T. Goslinski and L. Sobotta, *Nanomaterials*, 2020, **10**, 387.
17 A. Weir, P. Westerhoff, L. Fabricius, K. Hristovski and N. Von Goetz, *Environ. Sci. Technol.*, 2012, **46**, 2242–2250.
18 M. Bartoszewska, E. Adamska, A. Kowalska and B. Grobelna, *Molecules*, 2023, **28**, 645.
19 L. C. Mohr, A. P. Capelezzo, C. R. D. M. Baretta, M. A. P. M. Martins, M. A. Fiori and J. M. M. Mello, *Polym. Test.*, 2019, **77**, 105867.
20 Titanium Dioxide Nanomaterials Market Size & Industry Report, 2025-2033, **https://www.globalgrowthinsights.com/market-reports/titanium-dioxide-nanomaterials-market-106008**, accessed April 8, 2025.
21 S. Hamad, C. R. A. Catlow, S. M. Woodley, S. Lago and J. A. Mejías, *J. Phys. Chem. B*, 2005, **109**, 15741–15748.
22 M. Cargnello, T. R. Gordon and C. B. Murray, *Chem. Rev.*, 2014, **114**, 9319–9345.
23 A. Torres-Carbajal, S. Herrera-Velarde and R. Castañeda-Priego, *Phys. Chem. Chem. Phys.*, 2015, **17**, 19557–19568.
24 B. Faure, G. Salazar-Alvarez, A. Ahniyaz, I. Villaluenga, G. Berriozabal, Y. R. De Miguel and L. Bergström, *Sci. Technol. Adv. Mater.*, 2013, **14**, 023001.
25 S. Shrestha, B. Wang and P. Dutta, *Adv. Colloid Interface Sci.*, 2020, **279**, 102162.
26 D. Gentili and G. Ori, *Nanoscale*, 2022, **14**, 14385–14432.
27 P. Pal, in *Industrial Water Treatment Process Technology*, ed. P. Pal, Butterworth-Heinemann, 2017, pp. 145–171.
28 M. Hu, J. Zhou, Y. Li, X. Zhuo and D. Jing, *Chem. Eng. Sci.*, 2021, **246**, 116977.
29 M. A. Rahman, S. M. M. Hasnain, S. Pandey, A. Tapalova, N. Akylbekov and R. Zairov, *ACS Omega*, 2024, **9**(30), 32328–32349.
30 A. S. Almusallam, Y. M. Abdulraheem, M. Shahat and P. Korah, *J. Dispersion Sci. Technol.*, 2012, **33**, 728–738.
31 I. Fasaki, K. Siamos, M. Arin, P. Lommens, I. Van Driessche, S. C. Hopkins, B. A. Glowacki and I. Arabatzis, *Appl. Catal., A*, 2012, **411–412**, 60–69.
32 M. Kuo, S. Chang, P. Hsieh, Y. Huang and C. Li, *J. Am. Ceram. Soc.*, 2016, **99**, 445–451.
33 T. Yang, S. Chang, C. Li and P. Huang, *J. Am. Ceram. Soc.*, 2017, **100**, 56–64.
34 Y.-J. Yang, A. V. Kelkar, X. Zhu, G. Bai, H. T. Ng, D. S. Corti and E. I. Franses, *J. Colloid Interface Sci.*, 2015, **450**, 434–445.
35 T. Berglez, K. Kogej and J. Reščič, *J. Mol. Liq.*, 2023, **386**, 122464.
36 S. Monteiro, A. Dias, A. M. Mendes, J. P. Mendes, A. C. Serra, N. Rocha, J. F. J. Coelho and F. D. Magalhães, *Prog. Org. Coat.*, 2014, **77**, 1741–1749.
37 G. Garnweitner, H. O. Ghareeb and C. Grote, *Colloids Surf., A*, 2010, **372**, 41–47.
38 J. Y. Kao and W. T. Cheng, *ACS Omega*, 2020, **5**, 1832–1839.
39 I. M. Mahbubul, E. B. Elcioglu, R. Saidur and M. A. Amalina, *Ultrason. Sonochem.*, 2017, **37**, 360–367.
40 S. H. Othman, S. Abdul Rashid, T. I. Mohd Ghazi and N. Abdullah, *J. Nanomater.*, 2012, **2012**, 1–10.
41 J. Qi, Y. Y. Ye, J. J. Wu, H. T. Wang and F. T. Li, *Water Sci. Technol.*, 2013, **67**, 147–151.
42 J. Lee, S. L. Bartelt-Hunt, Y. Li and E. J. Gilrein, *Chemosphere*, 2016, **154**, 187–193.
43 R. A. French, A. R. Jacobson, B. Kim, S. L. Isley, R. L. Penn and P. C. Baveye, *Environ. Sci. Technol.*, 2009, **43**, 1354–1359.
44 M. Namakka, Md. R. Rahman, K. A. M. B. Said, M. Abdul Mannan and A. M. Patwary, *Environ. Nanotechnol., Monit. Manage.*, 2023, **20**, 100900.
45 I. Arora, H. Chawla, A. Chandra, S. Sagadevan and S. Garg, *Inorg. Chem. Commun.*, 2022, **143**, 109700.
46 M. M. Rashid, B. Simončič and B. Tomšič, *Surf. Interfaces*, 2021, **22**, 100890.
47 V. Kumaravel, K. M. Nair, S. Mathew, J. Bartlett, J. E. Kennedy, H. G. Manning, B. J. Whelan, N. S. Leyland and S. C. Pillai, *Chem. Eng. J.*, 2021, **416**, 129071.
48 M. Schutte-Smith, E. Erasmus, R. Mogale, N. Marogoa, A. Jayiya and H. G. Visser, *J. Coat. Technol. Res.*, 2023, **20**, 789–817.
49 C. Ayappan, S. K. Kannan, T. Ochiai, X. Zhang, R. Xing, S. Liu and A. Fujishima, *Trends Chem.*, 2025, **7**, 134–148.
50 A. A. Haidry, W. Yucheng, Q. Fatima, A. Raza, L. Zhong, H. Chen, C. R. Mandebvu and F. Ghani, *TrAC, Trends Anal. Chem.*, 2024, **170**, 117454.
51 J. Musial, R. Krakowiak, D. T. Mlynarczyk, T. Goslinski and B. J. Stanisz, *Nanomaterials*, 2020, **10**, 1110.
52 T. Ayorinde and C. M. Sayes, *J. Hazard. Mater. Lett.*, 2023, **4**, 100085.
53 H. Shi, R. Magaye, V. Castranova and J. Zhao, *Part. Fibre Toxicol.*, 2013, **10**, 15.
54 H. Zhang and J. F. Banfield, *Chem. Rev.*, 2014, **114**, 9613–9644.
55 M. Gopal, W. J. Moberly Chan and L. C. De Jonghe, *J. Mater. Sci.*, 1997, **32**, 6001–6008.
56 U. Müller, *Inorganic Structural Chemistry*, Wiley, 1st edn, 2006.
57 K. Momma and F. Izumi, *J. Appl. Crystallogr.*, 2011, **44**, 1272–1276.
58 J. F. Banfield and D. R. Veblen, *Am. Mineral.*, 1992, **77**, 545–557.

59 S. I. Sadia, Md. K. H. Shishir, S. Ahmed, A. R. Aidid, Md. M. Islam, Md. M. Rana, S. Md. Al-Reza and Md. A. Alam, *S. Afr. J. Chem. Eng.*, 2024, **50**, 51–64.
60 R. Chandoliya, S. Sharma, V. Sharma, R. Joshi and I. Sivanesan, *Plants*, 2024, **13**, 2964.
61 A. Kumar, *Nano*, 2018, **6**, 1.
62 R. S. B. Shivani, A. Bindu and S. P. Sajankila, *Nano-Struct. Nano-Objects*, 2025, **41**, 101455.
63 D. R. Eddy, D. Rahmawati, M. D. Permana, T. Takei, S. Solihudin, A. R. Noviyanti and I. Rahayu, *Inorg. Chem. Commun.*, 2024, **165**, 112531.
64 N. E. Sunny, S. S. Mathew, N. Chandel, P. Saravanan, R. Rajeshkannan, M. Rajasimman, Y. Vasseghian, N. Rajamohan and S. V. Kumar, *Chemosphere*, 2022, **300**, 134612.
65 N. Abid, A. M. Khan, S. Shujait, K. Chaudhary, M. Ikram, M. Imran, J. Haider, M. Khan, Q. Khan and M. Maqbool, *Adv. Colloid Interface Sci.*, 2022, **300**, 102597.
66 N. Baig, I. Kammakakam and W. Falath, *Mater. Adv.*, 2021, **2**, 1821–1871.
67 N. Thakur, N. Thakur, A. Kumar, V. K. Thakur, S. Kalia, V. Arya, A. Kumar, S. Kumar and G. Z. Kyzas, *Sci. Total Environ.*, 2024, **914**, 169815.
68 D. Fattakhova-Rohlfing, A. Zaleska and T. Bein, *Chem. Rev.*, 2014, **114**, 9487–9558.
69 L. Wang and T. Sasaki, *Chem. Rev.*, 2014, **114**, 9455–9486.
70 X. Wang, Z. Li, J. Shi and Y. Yu, *Chem. Rev.*, 2014, **114**, 9346–9384.
71 M. M. Mozael, Z. Dong, A. M. Pennington, F. E. Celik, B. H. Kear and S. D. Tse, *Powder Technol.*, 2024, **431**, 119058.
72 B. Derjaguin and L. Landau, *Prog. Surf. Sci.*, 1993, **43**, 30–59.
73 E. J. W. Verwey, *J. Phys. Chem.*, 1947, **51**, 631–636.
74 M. Elimelech, *Particle Deposition and Aggregation: Measurement, Modelling, and Simulation*, Butterworth-Heinemann, Woburn, 1998.
75 C. A. Silvera Batista, R. G. Larson and N. A. Kotov, *Science*, 2015, **350**, 1242477.
76 V. Agmo Hernández, *ChemTexts*, 2023, **9**, 10.
77 J. Kim, X.-H. Pham, H. Chang, B. S. Son, E. Hahm, S. H. Lee, W.-Y. Rho and B.-H. Jun, in *Nanotechnology for Bioapplications*, ed. B.-H. Jun, Springer Singapore, Singapore, 2021, vol. 1309, pp. 23–40.
78 E. Piacenza, A. Presentato and R. J. Turner, *Crit. Rev. Biotechnol.*, 2018, **38**, 1137–1156.
79 I. Sogami and N. Ise, *J. Chem. Phys.*, 1984, **81**, 6320–6332.
80 W. Zhang, in *Nanomaterial*, ed. D. G. Capco and Y. Chen, Springer Netherlands, Dordrecht, 2014, vol. 811, pp. 19–43.
81 N. M. Kovalchuk, D. Johnson, V. Sobolev, N. Hilal and V. Starov, *Adv. Colloid Interface Sci.*, 2019, **272**, 102020.
82 M. Elimelech, J. Gregory, X. Jia and R. A. Williams, in *Particle Deposition & Aggregation*, Elsevier, 1995, pp. 33–67.
83 S. V. Sokolov, K. Tschulik, C. Batchelor-McAuley, K. Jurkschat and R. G. Compton, *Anal. Chem.*, 2015, **87**, 10033–10039.
84 A. Brunelli, A. Foscari, G. Basei, G. Lusvardi, C. Bettiol, E. Semenzin, A. Marcomini and E. Badetti, *Sci. Total Environ.*, 2022, **829**, 154658.
85 Z. Guo, J. Xiong, M. Yang, S. Xiong, J. Chen, Y. Wu, H. Fan, L. Sun, J. Wang and H. Wang, *J. Alloys Compd.*, 2010, **493**, 362–367.
86 N. Kallay, T. Preočanin, D. Kovačević, J. Lützenkirchen and E. Chibowski, *Croat. Chem. Acta*, 2010, **83**, 357–370.
87 G. A. Parks, *Chem. Rev.*, 1965, **65**, 177–198.
88 T. Degabriel, E. Colaço, R. F. Domingos, K. El Kirat, D. Brouri, S. Casale, J. Landoulsi and J. Spadavecchia, *Phys. Chem. Chem. Phys.*, 2018, **20**, 12898–12907.
89 N.-Y. Joo, J. Lee, S. J. Kim, S. H. Hong, H. M. Park, W. S. Yun, M. Yoon and N. W. Song, *J. Nanosci. Nanotechnol.*, 2013, **13**, 6153–6159.
90 X. Liu, G. Chen and C. Su, *J. Colloid Interface Sci.*, 2011, **363**, 84–91.
91 A. Marucco, E. Aldieri, R. Leinardi, E. Bergamaschi, C. Riganti and I. Fenoglio, *Materials*, 2019, **12**, 3833.
92 S. Sen, V. Govindarajan, C. J. Pelliccione, J. Wang, D. J. Miller and E. V. Timofeeva, *ACS Appl. Mater. Interfaces*, 2015, **7**, 20538–20547.
93 I. Benammar, R. Salhi, J.-L. Deschanvres and R. Maalej, *IEEE Trans. Nanobiosci.*, 2017, **16**, 718–726.
94 S. Phromma, K. Injun, S. A-sachart, T. Wutikhun, U. Supcharoengoon, W. Kangwansupamonkon, T. Eksangsri and C. Sapcharoenkun, *J. Mol. Liq.*, 2023, **390**, 123032.
95 M. P. L. Sentis, N. Feltin, N. Lambeng, G. Lemahieu, G. Brambilla, G. Meunier and C. Chivas-Joly, *J. Nanopart. Res.*, 2024, **26**, 55.
96 W. Stumm and J. J. Morgan, *Aquatic Chemistry: Chemical Equilibria and Rates in Natural Waters*, John Wiley & Sons, Inc, New York Chichester Brisbane Toronto SIngapore, 3rd edn, 1996.
97 M. Kosmulski, *J. Colloid Interface Sci.*, 2011, **353**, 1–15.
98 M. Baalousha, Y. Nur, I. Römer, M. Tejamaya and J. R. Lead, *Sci. Total Environ.*, 2013, **454–455**, 119–131.
99 F. Gambinossi, S. E. Mylon and J. K. Ferri, *Adv. Colloid Interface Sci.*, 2015, **222**, 332–349.
100 H. Heinz, C. Pramanik, O. Heinz, Y. Ding, R. K. Mishra, D. Marchon, R. J. Flatt, I. Estrela-Lopis, J. Llop, S. Moya and R. F. Ziolo, *Surf. Sci. Rep.*, 2017, **72**, 1–58.
101 D. Myers, *Surfactant Science and Technology*, Wiley, 1st edn, 2005.
102 N. Filipović-Vinceković and V. Tomašić, in *Encyclopedia of Surface and Colloid Science*, Dekker, New York Basel, 2002.
103 S. M. Shaban, J. Kang and D.-H. Kim, *Compos. Commun.*, 2020, **22**, 100537.
104 R. Zhang and P. Somasundaran, *Adv. Colloid Interface Sci.*, 2006, **123–126**, 213–229.
105 P. K. Das, A. K. Mallik, R. Ganguly and A. K. Santra, *J. Mol. Liq.*, 2018, **254**, 98–107.
106 P. K. Das, A. K. Mallik, R. Ganguly and A. K. Santra, *Int. Commun. Heat Mass Transfer*, 2016, **75**, 341–348.
107 C. R. C. Hak, D. N. E. Fatanah, Y. Abdullah and M. Y. M. Sulaiman, *Int. J. Curr. Res. Sci. Eng. Technol.*, 2018, **1**, 172.
108 X. Chen, H. Cheng and J. Ma, *Powder Technol.*, 1998, **99**, 171–176.

109 X. Li, M. Yoneda, Y. Shimada and Y. Matsui, *Sci. Total Environ.*, 2017, **574**, 176–182.
110 R. S. Petryshyn, Z. M. Yaremko and M. N. Soltys, *Colloid J.*, 2010, **72**, 517–522.
111 T. Sato and S. Kohnosu, *J. Colloid Interface Sci.*, 1991, **143**, 434–439.
112 N. Veronovski, P. Andreozzi, C. La Mesa and M. Sfiligoj-Smole, *Surf. Coat. Technol.*, 2010, **204**, 1445–1451.
113 N. Veronovski, P. Andreozzi, C. La Mesa, M. Sfiligoj-Smole and V. Ribitsch, *Colloid Polym. Sci.*, 2010, **288**, 387–394.
114 A. Selmani, J. Lützenkirchen, K. Kučanda, D. Dabić, E. Redel, I. Delač Marion, D. Kralj, D. Domazet Jurašin and M. Dutour Sikirić, *Beilstein J. Nanotechnol.*, 2019, **10**, 1024–1037.
115 R. Zana, *Adv. Colloid Interface Sci.*, 2002, **97**, 205–253.
116 J. Schubert and M. Chanana, *Curr. Med. Chem.*, 2018, **25**, 4553–4586.
117 S. Elbasuney, *Curr. Med. Chem.*, 2017, **409**, 438–447.
118 K. Sato, J. Li, H. Kamiya and T. Ishigaki, *J. Am. Ceram. Soc.*, 2008, **91**, 2481–2487.
119 X. Sun, L. Ma, X. Tan, K. Wang and Q. Liu, *Colloids Surf., A*, 2020, **603**, 125195.
120 S. Liufu, H. Xiao and Y. Li, *J. Colloid Interface Sci.*, 2005, **281**, 155–163.
121 S. Fazio, J. Guzmán, M. T. Colomer, A. Salomoni and R. Moreno, *J. Eur. Ceram. Soc.*, 2008, **28**, 2171–2176.
122 H.-Y. Tsai, S.-J. Chang, T.-Y. Yang and C.-C. Li, *Ceram. Int.*, 2018, **44**, 5131–5138.
123 F. Karakaş and M. S. Çelik, *Colloids Surf., A*, 2013, **434**, 185–193.
124 M. J. Cran, G. E. Morris and L. Britcher, *Colloids Surf., A*, 2024, **684**, 133027.
125 W.-B. Tsai, J.-Y. Kao, T.-M. Wu and W.-T. Cheng, *J. Nanopart.*, 2016, **2016**, 1–9.
126 B. Peng, Y. Huang, L. Chai, G. Li, M. Cheng and X. Zhang, *J. Cent. South Univ. Technol.*, 2007, **14**, 490–495.
127 S. Salou, C.-M. Cirtiu, D. Larivière and N. Fleury, *Anal. Bioanal. Chem.*, 2020, **412**, 1469–1481.
128 T. C. Rezende, J. C. M. Silvestre, P. V. Mendonça, J. Moniz, A. C. Serra and J. F. J. Coelho, *Prog. Org. Coat.*, 2022, **165**, 106734.
129 B. P. Singh, S. Nayak, S. Samal, S. Bhattacharjee and L. Besra, *Appl. Surf. Sci.*, 2012, **258**, 3524–3531.
130 J. Jukić, T. Juračić, E. Josić, D. Namjesnik and T. Begović, *Adsorption*, 2024, **30**, 251–264.
131 K. Deshmukh, J. Ahmad, G. Joshi, M. B. Ahamed and M. B. Hägg, *J. Polym. Res.*, 2014, **21**, 393.
132 F. H. Haghighi, M. Mercurio, S. Cerra, T. Alberto Salamone, R. Bianymotlagh, C. Palocci, V. R. Spica and I. Fratoddi, *J. Mater. Chem. B*, 2023, **11**, 2334–2366.
133 L. Hallam, A. E. Papasergio, M. Lessio and J. Veliscek-Carolan, *J. Colloid Interface Sci.*, 2021, **600**, 719–728.
134 Y. Mou, K. M. Lü and D. M. Gao, *Adv. Mater. Res.*, 2011, **356–360**, 476–479.
135 E. Alebrahim, Md. S. Rahaman and C. Moreau, *Coatings*, 2022, **12**, 1764.
136 P. Rouster, M. Pavlovic and I. Szilagyi, *J. Phys. Chem. B*, 2017, **121**, 6749–6758.
137 F. Sallem, L. Villatte, P.-M. Geffroy, G. Goglio and C. Pagnoux, *Colloids Surf., A*, 2020, **602**, 125167.
138 C.-C. Li, S.-J. Chang and M.-Y. Tai, *Mater. Chem. Phys.*, 2011, **131**, 400–405.
139 V. Vaiano, O. Sacco, D. Sannino, W. Navarra, C. Daniel and V. Venditto, *J. Photochem. Photobiol., A*, 2017, **336**, 191–197.
140 J. M. Pettibone, D. M. Cwiertny, M. Scherer and V. H. Grassian, *Langmuir*, 2008, **24**, 6659–6667.
141 S. Lebrette, C. Pagnoux and P. Abélard, *J. Colloid Interface Sci.*, 2004, **280**, 400–408.
142 Y. Safaei-Naeini, M. Aminzare, F. Golestani-Fard, F. Khorasanizadeh and E. Salahi, *Iran. J. Mater. Sci. Eng.*, 2012, **9**, 62–68.
143 Y. Liu, Z. Yu, S. Zhou and L. Wu, *J. Dispersion Sci. Technol.*, 2006, **27**, 983–990.
144 N. Nakayama and T. Hayashi, *Colloids Surf., A*, 2008, **317**, 543–550.
145 J. S. Taurozzi, V. A. Hackley and M. R. Wiesner, *Preparation of Nanoscale TiO2 Dispersions in an Environmental Matrix for Eco-Toxicological Assessment*, National Institute of Standards and Technology, 2013.
146 R. F. Domingos, N. Tufenkji and K. J. Wilkinson, *Environ. Sci. Technol.*, 2009, **43**, 1282–1286.
147 R. F. Domingos, C. Peyrot and K. J. Wilkinson, *Environ. Chem.*, 2010, **7**, 61–66.
148 M. Elimelech, *Water Res.*, 1992, **26**, 1–8.
149 S. Ottofuelling, F. Von Der Kammer and T. Hofmann, *Environ. Sci. Technol.*, 2011, **45**, 10045–10052.
150 G. Raza, M. Amjad, I. Kaur and D. Wen, *Environ. Sci. Technol.*, 2016, **50**, 8462–8472.
151 M. Luo, Y. Huang, M. Zhu, Y. Tang, T. Ren, J. Ren, H. Wang and F. Li, *J. Saudi Chem. Soc.*, 2018, **22**, 146–154.
152 M. Filella, J. Buffle and N. Parthasarathy, in *Encyclopedia of Analytical Science*, ed. P. Worsfold, A. Townshend and C. Poole, Elsevier, Oxford, 2nd edn, 2005, pp. 288–298.
153 Y. Chen, Q. Gao, W. Chen, F. Wu, Y. Yang, D. Werner, S. Tao and X. Wang, *Water Res.*, 2018, **135**, 85–94.
154 R. A. Mathew, G. Wu, Y. Zhang, S. Shakiba, Y. Yao, A.-L. Tsai and S. M. Louie, *Environ. Sci.: Nano*, 2021, **8**, 2165–2176.
155 F. Loosli, P. Le Coustumer and S. Stoll, *Environ. Sci.: Nano*, 2014, **1**, 154.
156 M. B. Romanello and M. M. Fidalgo de Cortalezzi, *Water Res.*, 2013, **47**, 3887–3898.
157 H. Wang, J. Qi, A. A. Keller, M. Zhu and F. Li, *Colloids Surf., A*, 2014, **450**, 161–165.
158 C.-E. Hsiung, H.-L. Lien, A. E. Galliano, C.-S. Yeh and Y. Shih, *Chemosphere*, 2016, **151**, 145–151.
159 B. J. R. Thio, D. Zhou and A. A. Keller, *J. Hazard. Mater.*, 2011, **189**, 556–563.
160 M. Erhayem and M. Sohn, *Sci. Total Environ.*, 2014, **470–471**, 92–98.
161 M. Erhayem and M. Sohn, *Sci. Total Environ.*, 2014, **468–469**, 249–257.

162 K. Danielsson, J. A. Gallego-Urrea, M. Hassellov, S. Gustafsson and C. M. Jonsson, *J. Nanopart. Res.*, 2017, **19**, 133.
163 S. Callegaro, D. Minetto, G. Pojana, D. Bilanicová, G. Libralato, A. Volpi Ghirardini, M. Hassellöv and A. Marcomini, *Ecotoxicol. Environ. Saf.*, 2015, **117**, 107–114.
164 J. A. Gallego-Urrea, J. P. Holmberg and M. Hassellöv, *Environ. Sci.: Nano*, 2014, **1**, 181–189.
165 F. Loosli, P. Le Coustumer and S. Stoll, *Water Res.*, 2013, **47**, 6052–6063.
166 F. Loosli, P. Le Coustumer and S. Stoll, *Sci. Total Environ.*, 2015, **535**, 28–34.
167 M. Feng, C. Gu, C. Bao, X. Chen, H. Yan, Z. Shi, X. Liu and Q. Lin, *RSC Adv.*, 2018, **8**, 34397–34407.
168 D. Lin, S. Drew Story, S. L. Walker, Q. Huang and P. Cai, *Water Res.*, 2016, **104**, 381–388.
169 D. Lin, S. D. Story, S. L. Walker, Q. Huang, W. Liang and P. Cai, *Environ. Pollut.*, 2017, **228**, 35–42.
170 X. Gao, A. Middepogu, R. Deng, J. Liu, Z. Hao and D. Lin, *Sci. Total Environ.*, 2019, **694**, 133778.
171 T. Du, R. Meng, L. Qian, Z. Wang, T. Li and L. Wu, *Water Res.*, 2024, **249**, 120990.
172 Y. Zhang, X. Li, J. Du, L. Pu and S. Chen, *Desalin. Water Treat.*, 2021, **209**, 334–341.
173 A. S. Adeleye and A. A. Keller, *Environ. Sci. Technol.*, 2016, **50**, 12258–12265.
174 J. P. Paques, E. van der Linden, C. J. M. van Rijn and L. M. C. Sagis, *Adv. Colloid Interface Sci.*, 2014, **209**, 163–171.
175 S. N. Pawar and K. J. Edgar, *Biomacromolecules*, 2011, **12**, 4095–4103.
176 X. Gao, H. Zhang, X. Zhang, C. Zhang, C. Mao, S. Shan, F. Wei, M. Mortimer and J. Fang, *Environ. Sci.: Nano*, 2025, **12**, 2177–2192.
177 X. Gao, R. Deng and D. Lin, *Environ. Pollut.*, 2020, **263**, 114608.
178 X. Gao, K. Yang and D. Lin, *Sci. Total Environ.*, 2021, **778**, 146446.
179 X. Huangfu, Y. Xu, C. Liu, Q. He, J. Ma, C. Ma and R. Huang, *Chemosphere*, 2019, **219**, 766–783.
180 L. Xu, M. Xu, R. Wang, Y. Yin, I. Lynch and S. Liu, *Small*, 2020, **16**, 2003691.
181 I. Erceg, V. Strasser, N. Somers, M. Jurković, J. Kontrec, D. Kralj, R. Barbir, I. V. Vrček, M. Lasgorceix, A. Leriche and M. D. Sikirić, *J. Mol. Liq.*, 2023, **383**, 122122.
182 W. McKinney, M. Jackson, T. M. Sager, J. S. Reynolds, B. T. Chen, A. Afshari, K. Krajnak, S. Waugh, C. Johnson, R. R. Mercer, D. G. Frazer, T. A. Thomas and V. Castranova, *Inhalation Toxicol.*, 2012, **24**, 447–457.
183 A. Morlando, V. Sencadas, D. Cardillo and K. Konstantinov, *Powder Technol.*, 2018, **329**, 252–259.
184 K. H. Leong, J. Q. Lee, A. A. Kumar, L. C. Sim and S. Pichiah, *Malays. J. Anal. Sci.*, 2019, **23**, 90–99.
185 Z. Li, H. He, X. Wang, C. Shou, M. Huang, S. Jin and X. Du, *Colloids Surf., A*, 2023, **664**, 131176.
186 F. Li, J. Jiang, L. Niu, J. Chen, Y. Zhang, Y. Wang, X. Li and Z. Zhang, *Prog. Org. Coat.*, 2024, **189**, 108321.
187 J. Singh, P. B. Hegde, S. Avasthi and P. Sen, *ACS Omega*, 2022, **7**, 7816–7824.
188 K. Ilić, A. Selmani, M. Milić, T. M. Glavan, E. Zapletal, M. Ćurlin, T. Yokosawa, I. V. Vrček and I. Pavičić, *J. Nanopart. Res.*, 2020, **22**, 71.
189 L. Kong, J. Sun, Y. Bao and Y. Meng, *Wear*, 2017, **376–377**, 786–791.
190 Y. Ye, H. Bruning, W. Liu, H. Rijnaarts and D. Yntema, *J. Photochem. Photobiol., A*, 2019, **371**, 216–222.
191 J. Ma, L. Zhang, Z. Fan, S. Sun, Z. Feng, W. Li and H. Ding, *J. Alloys Compd.*, 2023, **968**, 172127.
192 W. Ko, B. J. Cha, Y. D. Kim and H. O. Seo, *Catal. Today*, 2022, **403**, 47–57.
193 Y.-A. Leu, Y.-A. Lu, M.-H. Yeh, P.-T. Shih, S.-Y. Shen, K.-C. Ho and J.-J. Lin, *ACS Appl. Mater. Interfaces*, 2018, **10**, 38394–38403.
194 J. Park, S. Ham, S. Kim, M. Jang, J. Lee, S. Kim, D. Park, K. Lee, H. Kim, P. Kim and C. Yoon, *Indoor Air*, 2020, **30**, 925–941.